Boletim de Geociências da Petrobras

Faciological and petrological characterization of basic sills in the Picos-PI region, eastern portion of the Parnaíba Basin

Caracterização faciológica e petrológica das soleiras básicas da região de Picos-PI, porção leste da Bacia do Parnaíba

[1]Felipe Mature Ribeiro da Silva, [2]Carla Joana Santos Barreto, [2]Sara Gomes da Costa, [2]Jully Vivianne de Albuquerque Alves, [2]Aline Macrina da Silva, [3]Júlia Stefane da Silva Vieira
[1]Universidade Federal de Pernambuco, Recife, Pernambuco, Brasil, felipe.mature@ufpe.br (Autor correspondente)
[2]Universidade Federal de Pernambuco, Recife, Pernambuco, Brasil
[3]Universidade Federal da Paraíba, João Pessoa, Paraíba, Brasil

ABSTRACT

Two major basic magmatic events from the Mesozoic have been identified in the Parnaíba Basin. The first, associated with the Jurassic - Triassic boundary, is correlated with the Central Atlantic Magmatic Province (CAMP) and is represented in the basin by the Mosquito Formation. This event occurs mainly as lava flows and intrusions of dikes and sills in the western portion of the Basin. The second event is linked to the Cretaceous and is represented by the Sardinha Formation. It consists predominantly of intrusive rocks such as dikes and sills in the eastern part of the basin; however, its magmatic origin remains debated. This study aimed to characterize the intrusive rocks in the Picos region of the eastern Parnaíba Basin through facies identification and classification, detailed petrographic analysis of the bottom, core, and top sections, and major-element geochemistry. Dolerite sills were described and categorized into regular columnar facies characterized by cooling fractures and massive dolerite. Additionally, the rocks were subdivided into phaneritic and aphanitic types. Subophitic, intergranular, and granophyric textures were observed in the phaneritic dolerite, while the aphanitic ones exhibited porphyritic, intersertal, and intrafascicular textures, typical of rapid crystallization. Geochemically, the rocks were classified as basic to intermediate, metaluminous, high-TiO_2, and tholeiitic. These results indicate that the dolerite underwent distinct crystallization processes during emplacement, with the aphanitic types suggesting that aphanitic types experienced higher cooling rates. Based on petrographic and geochemical similarities with previous studies, we suggest that these rocks belong to the Sardinha Formation.

Keywords: Sardinha Formation, dolerite, sub-volcanic petrography.

RESUMO

Dois grandes eventos magmáticos básicos, ocorridos durante o Mesozoico, são identificados na Bacia Parnaíba. O primeiro, ocorrido dentro dos limites Juro-Triássico, é correlato à Província Magmática do Atlântico Central (CAMP), sendo expresso pela Formação Mosquito. Este evento ocorre principalmente como fluxos de lava e intrusões de diques e soleiras na porção oeste da bacia. O segundo evento, correspondente ao Cretáceo, é representado pela Formação Sardinha, a qual é expressa principalmente por rochas intrusivas, como diques e soleiras na parte leste da Bacia Parnaíba, cuja origem magmática ainda permanece em discussão. Dessa forma, este presente trabalho objetivou abordar as rochas intrusivas na região de Picos-PI, na porção leste da Bacia Parnaíba. A pesquisa inclui a identificação e classificação faciológica, além da análise petrográfica detalhada das porções de base, núcleo e topo, somada à geoquímica de elementos maiores dessas rochas. Foram descritas soleiras de doleritos, classificados faciologicamente em colunares regulares com fraturas por resfriamento e doleritos maciços, que foram subdivididos em faneríticos e afaníticos. Nos doleritos faneríticos, observou-se texturas subofítica, intergranular e granofírica, enquanto nos afaníticos exibem texturas porfirítica, intrafascicular e intersertal, típicas de cristalização acelerada. Não obstante, através da análise geoquímica, classificamos essas rochas como básicas a intermediárias, metaluminosas, alto TiO_2 e toleíticas. Portanto, os resultados indicam que os doleritos passaram por diferentes processos de cristalização durante seu emplacement, em que os doleritos afaníticos sofreram com rápidas taxas de resfriamento. Além disso, através da semelhança petrográfica e geoquímica entre os trabalhos anteriores e nossas amostras, assumimos que estas rochas fazem parte da Formação Sardinha.

Palavras-chave: Formação Sardinha, dolerito, petrografia subvulcânica.

Recebido: 25 de agosto de 2025 | Recebido no formato de revisão: 28 de outubro de 2025 | Aceito: 30 de dezembro de 2025 | Disponível online: 23 de fevereiro de 2026

DOI: https://doi.org/10.70369/h8gfjv76

1. INTRODUCTION

Magmatism on global scales is known as LIPs (Large Igneous Provinces). It represents important episodes in Earth's geological evolution, generating large extrusive flows fed by intrusions over a short span of time (Coffin and Eldholm, 1992; 1994; 2001). Extensive basaltic flows, fed by intrusive bodies, preceded the onset of Gondwana breakup during the Mesozoic Era. These events were initiated by combination of continental stress and high mantle activity, such as mantle plumes. Two significant events are recognized: the Central Atlantic Magmatic Province (CAMP) and the Paraná-Etendeka Magmatic Province (PEMP) (Sial, 1974; Bellieni et al., 1984; Marzoli et al., 1999). The first, of Triassic-Jurassic age, is classically correlated with the Central Atlantic Magmatic Province (CAMP) and is represented in the basin by the Mosquito Formation, which occurs mainly as flows and intrusions in the western portion. The second event is linked to the Cretaceous, represented by the Sardinha Formation. It predominantly manifests as intrusions (sills and dykes) in the eastern portion of the basin, notably in the Picos region, Piauí (Sial, 1974; Fodor et al., 1990; Baksi and Archibald, 1997; Vaz et al., 2007; Heilbron et al., 2018; Oliveira et al., 2018; Fornero et al., 2023; Silva et al., 2024).

Nonetheless, several studies have shown the chemical differences between the Mosquito and Sardinha formations. However, these studies indicate significant chemical variation among the rocks of the Sardinha Formation, which is not observed in the rocks of the Mosquito Formation (Bellieni et al., 1990; Fodor et al., 1990; Marzoli et al., 1999; Heilbron et al., 2018; Oliveira et al., 2018; Macêdo Filho and Hollanda, 2022; Macêdo Filho et al., 2023).

Regarding the Parnaíba Basin, a substantial body of literature is available focusing on its sedimentary, structural, paleontological, and petrological characteristics (Sial, 1974; Caputo, 1985; Milani and Zalán, 1999; Arai, 2014; Heilbron et al., 2018). Meanwhile, studies related to the physical volcanology approach, such as facies analysis (Cas and Wright, 1987; McPhie, 1993; Jerram, 2002), have been little explored in the Parnaíba Basin.

Meanwhile, studies of volcanic rocks, exemplified in the Paraná Basin, extensively utilize the physical volcanology approach, including facies analysis (Barreto et al., 2014; Rossetti et al., 2014; Sarmento et al., 2017; Fornero et al., 2023; Waichel et al., 2024). However, a significant gap remains concerning facies-related studies of these surface-exposed igneous rocks for the Parnaíba Basin and the Sardinha Formation. Considering the relevance of this approach, this study aims to provide a pioneering analysis of the eastern portion of the basin by integrating facies analysis with detailed petrographic characterization of the bottom, core, top, and geochemistry of the whole rock.

In this context, the primary objective of this study is to integrate previously described facies features (Silva et al., 2024) with a detailed petrographic description of the bottom, core, and top of dolerite sills in the Picos region, Piauí. This integration will enable the development of a descriptive model that can be applied to other regions with intrusive igneous successions. Moreover, this research aims to contribute new geochemical data, enabling the identification of the magmatic formation to which these sills belong, based on petrographic and geochemical evidence. Ultimately, the study aims to conduct a comparative analysis of the geochemical data from the eastern Parnaíba Basin with those available in the literature for the PEMP, CAMP, and EQUAMP provinces. Moreover, to contribute to a future subdivision of the Sardinha Formation, which demonstrates substantial differences in geochemical data.

2. GEOLOGICAL CONTEXT

The breakup of the South American Platform from the southern part of the Gondwana Supercontinent was preceded by a major magmatic event known as the Central Atlantic Magmatic Province (CAMP). CAMP was a vast continental flood basalt province that affected large portions of North and South America, as well as parts of Europe and West Africa (Ernesto et al., 2003).

This magmatism covered an area exceeding 4 million km² and is expressed through lava flows, sills, and dyke swarms, dated to approximately 200 Ma (Marzoli et al., 1999). This event is recognized in four Brazilian intracratonic basins: the Amazon Basin, the Solimões Basin, the Parecis Basin, and the Early Jurassic phase of the Parnaíba Basin, represented by the Mosquito Formation (Marzoli et al., 1999; Hames et al., 2000; 2003; Miranda, 2014; Rezende et al., 2021; Waichel et al., 2024).

The initial phase of South Atlantic Ocean opening triggered another episode of widespread basaltic flows, primarily affecting the southern region of the South American Platform and the southwestern margin of Africa. This event is known as the Paraná-Etendeka Magmatic Province (PEMP) (~135 Ma) (Bellieni et al., 1984; Thomaz Filho et al., 2000; Ewart, 2004; Cioccari and Mizusaki, 2019). In Brazil, this province encompasses the Paraná Basin, which was covered by approximately 1.5 million km² of tholeiitic basaltic rocks, including lava flows, dyke swarms, and sills referred to as the Serra Geral Group (Rämö et al., 2016; Barreto et al., 2014; Rossetti et al., 2014; Oliveira et al., 2018).

The intracratonic Parnaíba Basin is predominantly located in the northeastern and northern regions of Brazil, covering an area exceeding 600,000 km² and

reaching depths of approximately 3,500 m (Góes and Feijó, 1994; Vaz et al., 2007; Pereira et al., 2012). This intracratonic basin developed during the stabilization phase of the South American Platform (Almeida and Carneiro, 2004), with sedimentation initiated in the late Precambrian to early Paleozoic (Vaz et al., 2007). The sedimentary formations deposited in the Parnaíba Basin were affected by these two events, the CAMP, represented by the Mosquito Formation (Jurassic) (Marzoli et al., 1999; Hames et al., 2000; 2003) and later by the Sardinha Formation (Cretaceous), commonly correlated to the PEMP (Bellieni et al., 1984; Thomaz Filho et al., 2000; Ewart, 2004), and more recently by the Central Atlantic Magmatic Province (EQUAMP) (Hollanda et al., 2018).

Góes and Feijó (1994) subdivided the Parnaíba Basin into five supersequences, deposited between the Paleozoic and Mesozoic eras. The first of these correlates to the Silurian period and is represented by the Serra Grande Group, which represents a transgressive-regressive sedimentary cycle (Vaz et al., 2007). The second supersequence is composed of the Canindé Group, consisting of sediments from tidal and storm cycles, shallow marine and fluvial, during the Devonian period (Vaz et al., 2007; Miranda, 2014). The Balsas Group represents the third supersequence and comprises clastic, carbonate, and shale rocks with high organic matter content. In addition, it also has high sedimentation exclusively continental and eolian, such as the Sambaíba Formation (Abrantes Júnior and Nogueira, 2013). Furthermore, during the Mesozoic, two magmatic pulses affected the Parnaíba Basin, both intrusive and extrusive, expressed as the Mosquito and Sardinha Formations, related to the openings of the North Atlantic (Triassic-Jurassic) and South Atlantic (Cretaceous), respectively (Bellieni et al., 1984; Thomaz Filho et al., 2000; Ewart, 2004). These magmatic pulses mainly affected the Canindé Group (Devonian), where the Sardinha Formation is mainly found, in the eastern portion of the Parnaíba Basin (Góes and Feijó, 1994; Marzoli et al., 1999; Milani and Zalán, 1999; Thomaz Filho et al., 2000; Vaz et al., 2007; Silva et al., 2024).

The Mosquito Formation is composed of basaltic rocks exposed in the western portion of the Parnaíba Basin, forming well-preserved lava flows that commonly exhibit amygdaloidal textures, occasionally interbedded with sandstones (Oliveira et al., 2018). In addition, the Mosquito Formation intrudes sequences of Silurian sedimentary rocks, as well as strata from the Middle Devonian - Early Carboniferous and Late Carboniferous - Early Triassic intervals (Vaz et al., 2007). The igneous unit of the Mosquito Formation is correlated with the Penatecaua Magmatism (210 - 201 Ma) (Mizusaki et al., 2002; Angelim et al., 2004; Zalán, 2004).

The Sardinha Formation is characterized in the Parnaíba Basin by the presence of dike intrusions and, to a lesser extent, small sills (Vaz et al., 2007). However, more recent studies have shown that the Sardinha Formation also occurs as extensive dolerite sills despite limited surface exposure and, in some cases, as basaltic lava flows (Heilbron et al., 2018; Oliveira et al., 2018; Silva et al., 2024). This formation is predominantly found in contact with Middle Devonian - Early Carboniferous sedimentary sequences, especially the Pimenteiras and Cabeças formations (Vaz et al., 2007; Miranda, 2014; Oliveira et al., 2018; Cioccari and Mizusaki, 2019; Silva et al., 2024).

Some studies associate the Sardinha Formation with the basaltic flows of the Serra Geral Group (137 - 127 Ma) (Thomaz Filho et al., 2000), whereas other authors challenge this correlation due to geographic distance, geochemical variation, and isotopic age discrepancies (Baksi and Archibald, 1997; Oliveira et al., 2018; Hollanda et al., 2018). The latter studies propose that the Sardinha Formation is instead related to a third magmatic event linked to the rifting of the equatorial Atlantic margin, known as the Equatorial Atlantic Magmatic Province (EQUAMP) (Figure 1) (Hollanda et al., 2018; Macêdo Filho and Hollanda, 2022; Macêdo Filho et al., 2023).

3. MATERIAL AND METHODS

The field-based data used in this study, which include the geological mapping of dolerite occurrences in Picos-PI and surrounding areas, as well as facies analysis along the igneous bodies, were previously described and published in Silva et al. (2024).

This current research builds upon these findings, focusing on detailed petrographic analysis of the base, core, and top of the two dolerite stratigraphic profiles. Following the fieldwork campaign that provided the samples, petrographic analysis was performed on 21 thin sections.

For geochemical analyses, seven rock samples were selected, crushed and pulverized at the Núcleo de Estudos Geoquímicos - Laboratório de Isotopos Estáveis (NEG-LABISE), Federal University of Pernambuco, Brazil. In the next step, the samples were oven-dried at 110 °C, and a portion of the dried material was placed in a muffle furnace at 1000 °C for two hours to determine the loss on ignition (LOI). Another portion of the dried sample was pressed into an aluminum capsule under 30 tons of force. The pressed pellets were sent to the NEG-Labise Laboratory for analysis using a Rigaku ZSX Primus II X-ray fluorescence spectrometer, equipped with a Rh tube and seven analyzing crystals. The oxide results were recalculated to 100% on an anhydrous basis (LOI-free) and are expressed as weight percent (%). The analytical results obtained (Table 1) were processed using the open-source software GCDkit 4.1 (Janoušek et al., 2006), from which geochemical diagrams were generated.

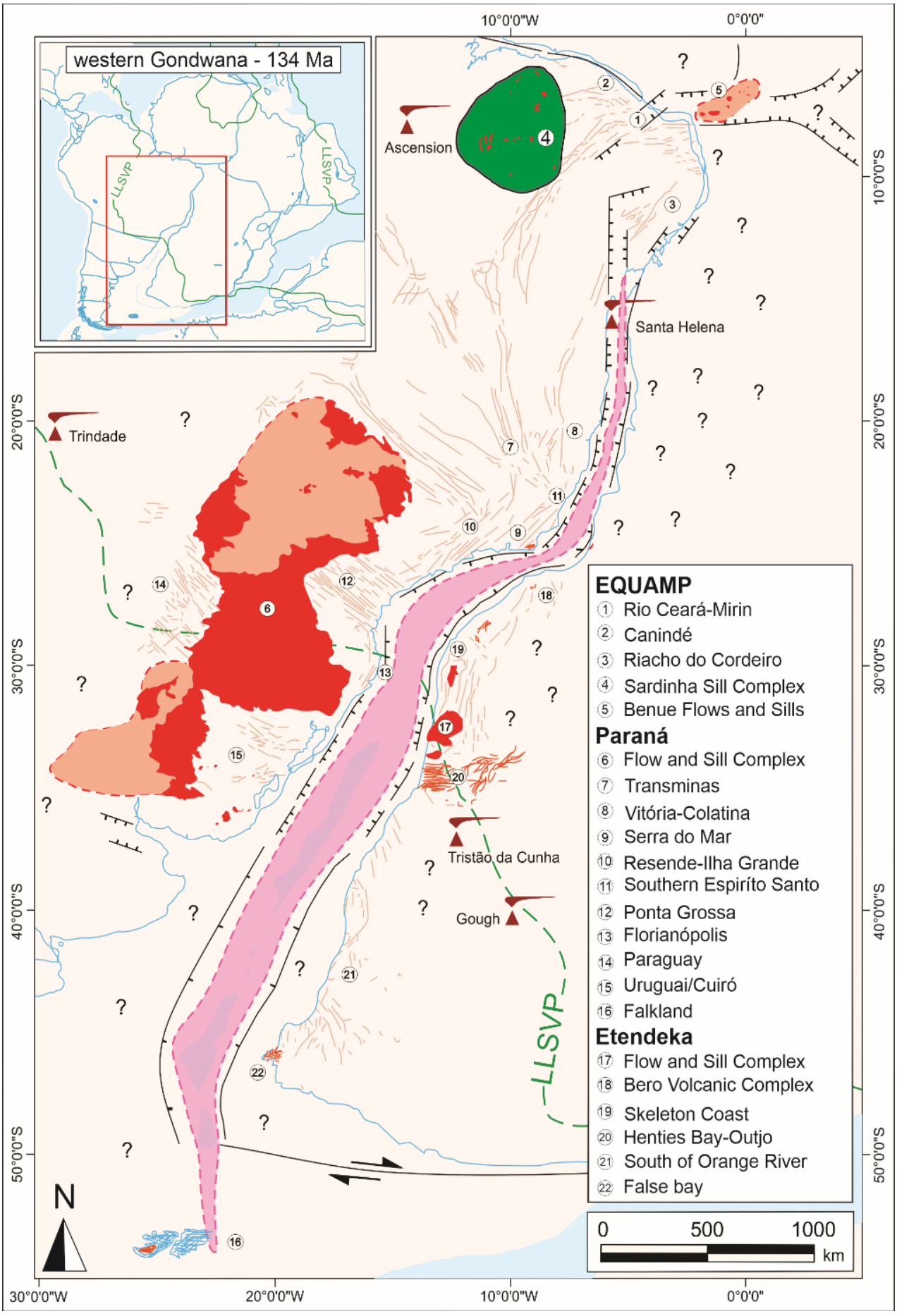

Figure 1. Reconstruction map of western Gondwana during the Cretaceous period, highlighting magmatic occurrences associated with LIPs (Macêdo Filho et al., 2023).

4. RESULTS

4.1. Field and outcrops aspects

The study area, located in Picos-PI and surrounding areas, is in the Parnaíba Basin (Figure 2A). Moreover, the first step of this work was the recognition and mapping of dolerites, in outcrops identified in previous works and new others (Figure 2B). Additionally, the point PI-21-40 is a new outcrop found and described in this work.

All of these rocks in the present study are observed as intrusions of medium to large sills, which intrude the Cabeças Formation (figures 3 and 4), sometimes with an observed contact below these sandstones in cross-section. It is important to note that sill outcrops on the surface, with an average height of 20 m to 100 m in length. These outcrops are found in road cuts (Figure 3E), mining companies (Figure 3B), and slabs (Figure 3F) with minor occurrences.

Furthermore, several different facies were observed in these rocks, making the use of lithofacies analysis an important tool, in addition to petrography and geochemistry analysis, to understand the emplacement of these rocks better. In the case of these differences regarding outcrops, size, facies, and rock characteristics, and to facilitate the work, we create a table that summarizes some important information (Table 1).

Table 1. Field and outcrops describe, as lithology types, textures, structures and facies code.

Lithology	Geometry	Facies code	Texture	Structure
Dolerite	Sill	Dpcv	Phaneritic	Vertical column disjunction
Dolerite		Dpm	Phaneritic	Massive
Dolerite		Dpfr	Phaneritic	Fractures
Dolerite		Dacv	Aphanitic	Vertical column disjunction
Dolerite		Dach	Aphanitic	Horizontal column disjunction

The lithological, structural, and textural characteristics of the dolerite sills are described in the investigated area (Figure 2) (Silva et al., 2024). However, the present work makes some modifications to the previous work cited above, as shown in Table 1. The main difference in dolerites is the grain and textures, because most dolerites are phaneritic, and less commonly, aphanitic.

Figure 3A represents the composite stratigraphic profile, which contains all dolerite classified as phaneritic, and the facies present in the whole profile, at the base, core, and top of these dolerites. The phaneritic dolerite profile comprises PI-21-05, PI-21-06, PI-21-07 and PI-21-34 (Figure 2B).

The phaneritic dolerites display fine to medium-grained textures, and the size of plagioclase crystals in these rocks ranges from 0.5 mm to 1 mm (Figure 3D and 3F). In contrast, pyroxenes are approximately 0.5 mm in size, with some submillimeter crystals of magnetite and rare iron sulfides, such as pyrite. Moreover, all of these dolerites are classified as phaneritic and exhibit different facies, including transverse fractures (*Dpfr*), massive dolerites (*Dpm*), and vertical columnar joints (*Dpcv*), with typical facies at the base, core, and top, respectively (Figure 3A). Furthermore, the secondary process involves the chemical interaction of fluids with dolerites, which recrystallize carbonates (Figure 3C) and oxidize the mafic minerals (Figure 3I). Moreover, physical weathering is evident in spheroidal exfoliation.

The second stratigraphic profile corresponds to rocks from a single outcrop in the region (PI-40), classified as an aphanitic (Figure 4A) with rare microphenocrysts of plagioclase embedded in an aphanitic groundmass (Figure 4F). This outcrop comprises a large sill with an average thickness of 20 m on average and some locations exceed 30 m and spread to 100 to 200 m, the microphenocrysts of plagioclase range in size 0.5 mm on average.

The basal portion of these dolerites is characterized by a massive internal aspect and typical regular vertical columnar jointing (*Dacv*), with fractures exhibiting polygonal shapes ranging from pentagonal to hexagonal in plan view (Figure 4D). The spacing between the columns is on the order of a few centim. The rocks exhibit physical weathering, such as spheroidal exfoliation (Figure 4G).

The intrusion core retains the massive structure and vertical columnar jointing (*Dacv*) observed at the base (Figure 4A), although the column spacing is larger. No macroscopic textural variations were noted in this section. The upper portion of the basaltic bodies is mainly characterized by regular horizontal fractures (*Dch*) (figures 4B and 4C), which distinguish this section from the rest of the outcrop.

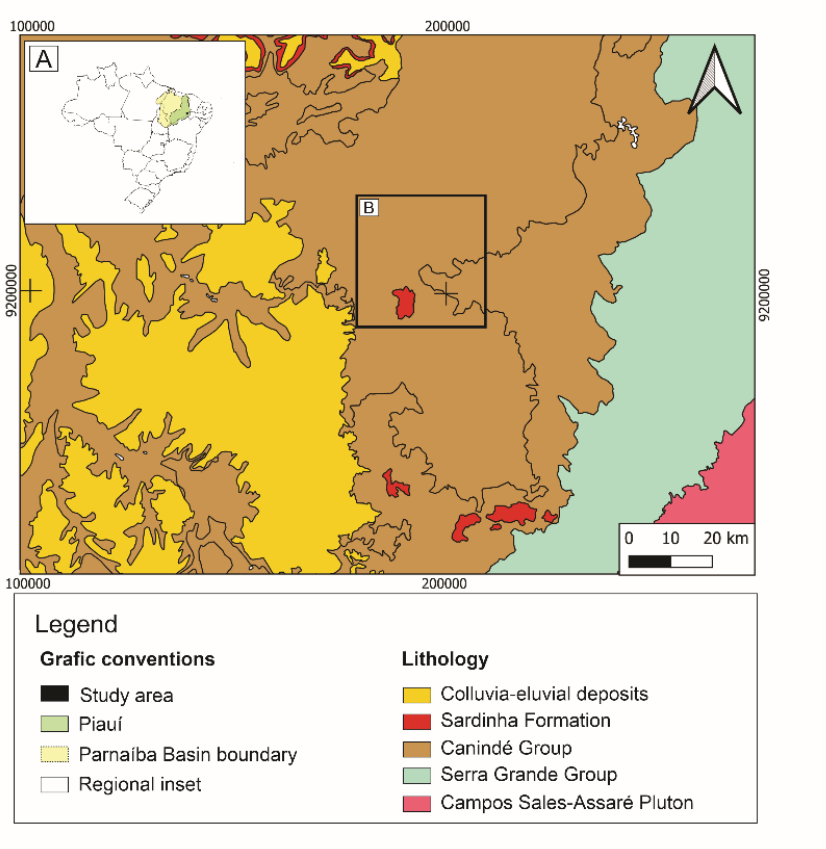

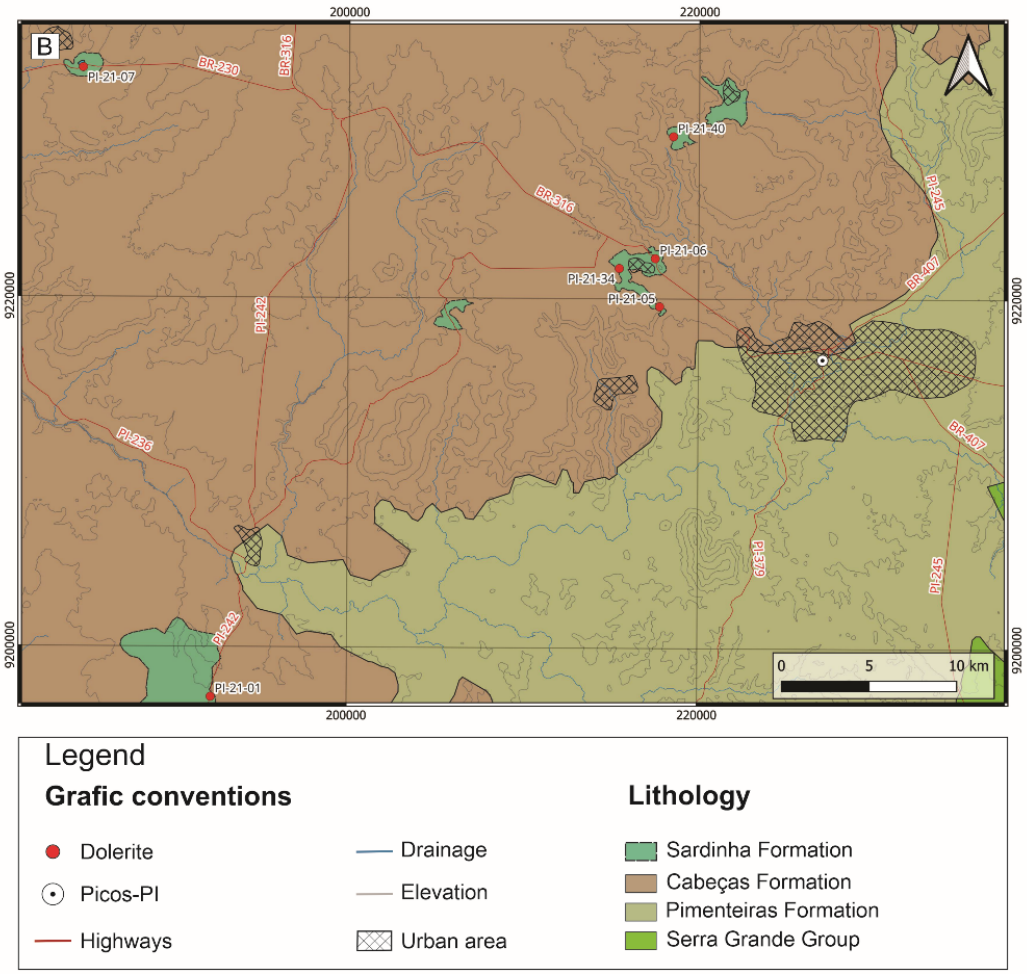

Figure 2. A. Regional geological map of the study area. **B.** Map of occurrences of the lithostratigraphic units present in the locality of Picos and surrounding areas. Modified after Angelim et al. (2004).

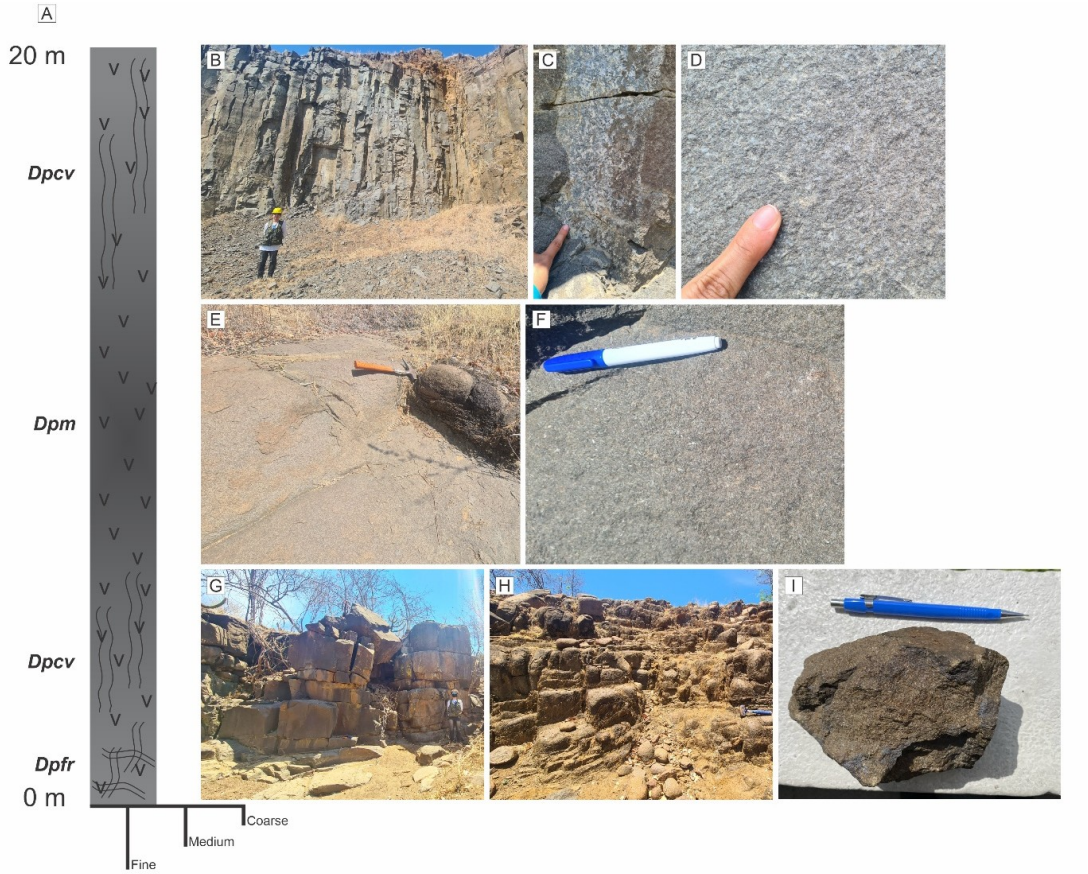

Figure 3. A. Composite stratigraphic profile of phaneritic dolerites. **B.** Large size of columnar jointing. **C.** Recrystallization of calcite in dolerite. **D.** Medium grain size of phaneritic rocks, with plagioclase laths and pyroxene crystals. **E.** Dolerites in slabs. **F.** Medium-grained slabs of dolerite. **G.** Phaneritic dolerite with horizontal and vertical fractures. **H.** Individual blocks generated by spheroidal exfoliation. **I.** Sample oxidizes of the Dpfr.

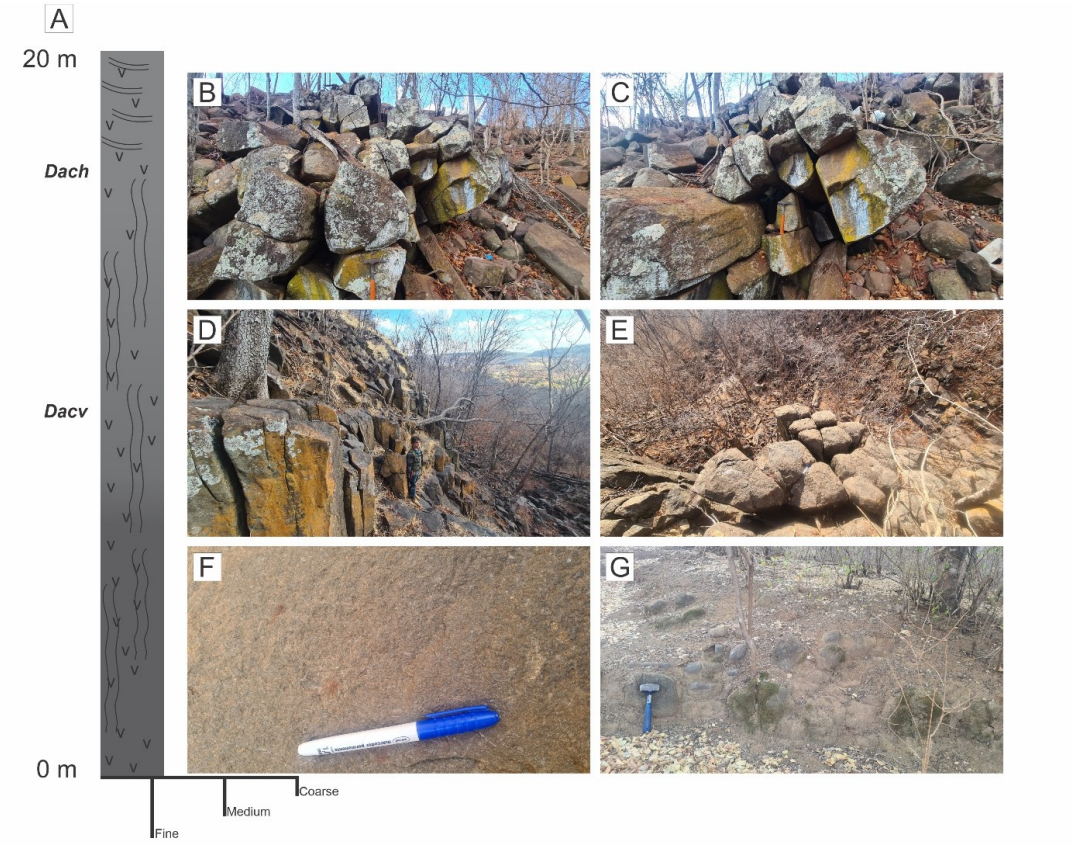

Figure 4. A. Profile of aphanitic dolerite and facies. **B.** and **C.** Polygonal shapes. **D.** Overview of outcrop. **E.** Plain view of outcrop showing the shapes of dolerite. **F.** Fine dolerite with laths of plagioclase embedded in the groundmass. **G.** Overview of weathering in outcrop with individual blocks generated by spheroidal exfoliation.

4.2. Petrographic implications

Petrographic analyses also showed differences between the phaneritic (Figure 5A) and aphanitic (Figure 6A) dolerite sills. These are holocrystalline, inequigranular rocks, with crystals reaching up to 1.5 mm among the plagioclase phenocrysts. Clinopyroxene crystals average 0.5 mm but can reach up to 1 mm in some cases. It is worth noting that the darker portions of the stratigraphic profiles comprise the facies with the least amount of groundmass, observed in the central portions of profile 1 (Figure 3), as shown in the photomicrographs of this portion (Figure 5G). Whereas in profile 2 (Figure 4), a greater amount of crystals relative to the groundmass is observed, also shown in the photomicrographs (Figure 6C).

Mineralogically, the dolerites are composed of plagioclase, clinopyroxene, and opaque minerals, including magnetite and ilmenite, with an accessory phase marked by apatite. In a rare case, a biotite crystal was observed enclosed within a plagioclase crystal (Figure 5B).

The plagioclase crystals are euhedral and exhibit a tabular or columnar habit, with the larger crystals displaying a columnar shape. Alteration of these minerals is observed mainly to sericite and carbonatization. Meanwhile, the clinopyroxene crystals are primarily subhedral, forming short prisms or very elongated crystals, and alteration is observed through oxidation of minerals.

4.2.1. Phaneritic dolerite

The rock is holocrystalline and inequigranular, with crystals ranging from <0.5 mm to 1.5 mm. It is mainly composed of plagioclase crystals (~80%), clinopyroxene (~15%), and opaque minerals (~5%) (Figure 5A). The accessory phase (<1%) is represented by minute crystals of biotite and apatite (Figure 5B).

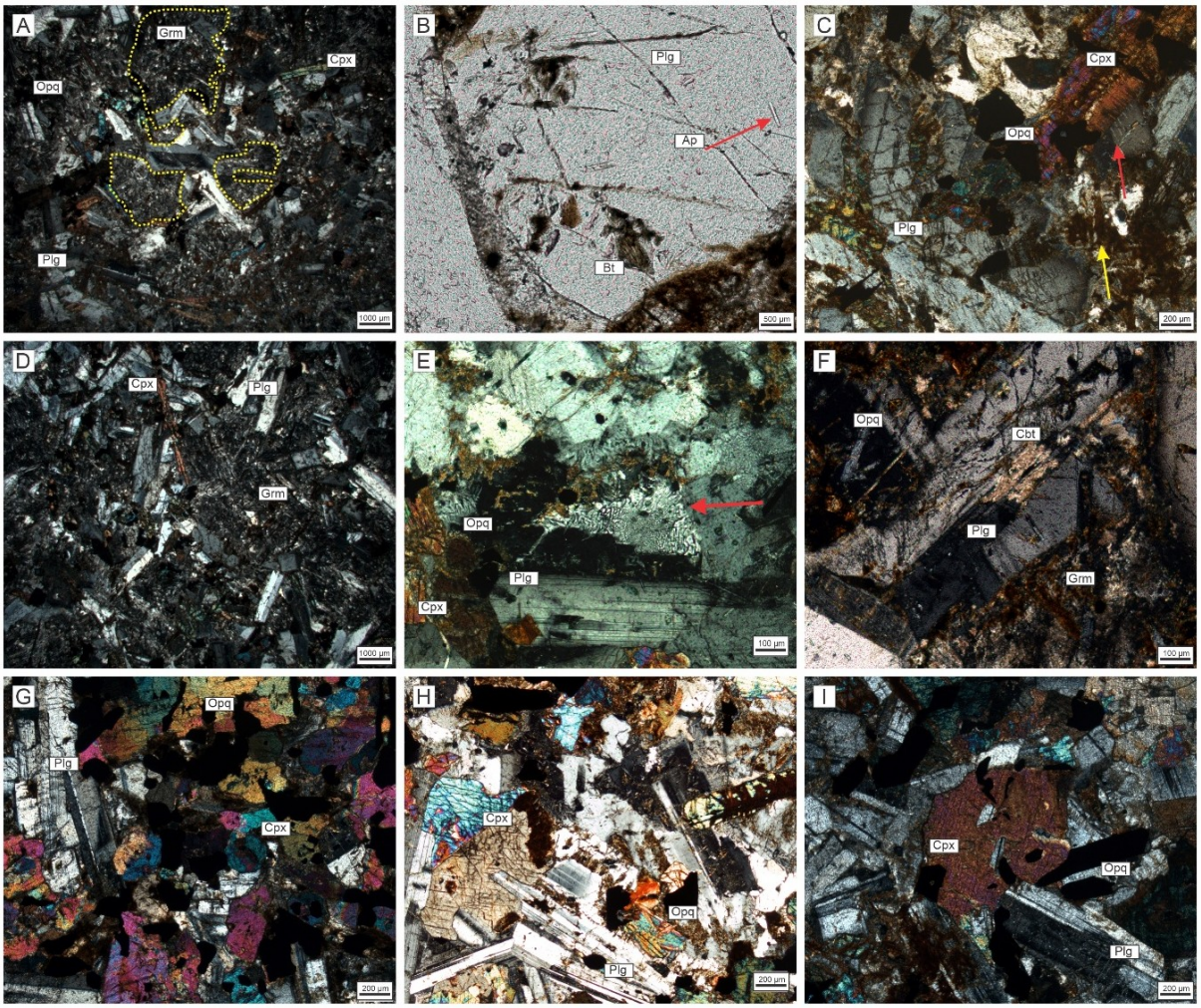

Figure 5. A. General petrographic aspect of the thin section under crossed polars**,** showing the central mineralogy. Note the isolated distribution of the groundmass**,** forming pockets between the crystals (detailed by the yellow dotted line). **B.** Accessory mineralogy observed under plane-polarized light, with apatite crystals included in the plagioclase phenocrysts (red arrow). **C.** Sericitization of plagioclase crystals (red arrow) and oxidation of clinopyroxene, under crossed polars. **D.** Shape of plagioclase and clinopyroxene crystals found in the rock, under crossed polars. **E.** Photomicrograph detail of the micrographic texture (red arrow) in crossed polars. **F.** Carbonatization of plagioclase crystals, under crossed polars. **G.** Intergranular texture, under crossed polars. Note the Skeletal opaque mineral, possibly ilmenite. **H.** Subophitic texture under crossed polars. **I.** Ophitic texture under crossed polars.

As products of alteration, sericitization of plagioclase crystals and oxidation of clinopyroxenes are observed (Figure 5C), in addition to opacitization of some clinopyroxene crystals. Processes such as carbonatization are also seen, mainly in plagioclase crystals (Figure 5F).

The plagioclase crystals are predominantly euhedral and tabular to lath-shaped. In contrast, the clinopyroxene crystals are euhedral to subhedral, forming short prisms to fine columnar crystals (Figure 5D). Furthermore, the opaque crystals are euhedral to subhedral and form tabular minerals with well-defined geometric shapes, such as squares and rectangles, and sometimes within skeletal forms, typical of ilmenite. In the central portions of the phaneritic dolerites (*Dpm*), the micrographic textures are also noteworthy, showing vermiform quartz crystals in feldspars (Figure 5E).

The groundmass is microcrystalline and is composed of a reddish-brown material with very fine crystals classified as feldspars (Figure 5A). It is important to emphasize that the groundmass found in these sills appears mainly in the base and top portions, in an isolated manner, forming pockets between the rock-forming crystals (Figure 5A).

The main texture found in the phaneritic dolerites is intergranular, defined by the clinopyroxene crystals located between the columnar plagioclase crystals (Figure 5G). Less commonly, the subophitic texture is also found, with plagioclase crystals partially enclosed within the clinopyroxene crystals (Figure 5H). We found only one occurrence of the ophitic texture, which includes the entire plagioclase crystal within the clinopyroxene (Figure 5I).

4.2.2. Aphanitic dolerite

The aphanitic dolerites are holocrystalline and inequigranular, with crystals reaching up to 1.5 mm in length. They are composed predominantly of plagioclase (~85%), clinopyroxene (~10%), and opaque minerals (~5%) (Figure 6A). The accessory phase consists of minute apatite crystals, which are included within the plagioclase phenocrysts. Alteration products are primarily observed through the oxidation of clinopyroxene crystals, and, at lower rates, the sericitization of plagioclase (Figure 6B).

The plagioclase crystals represent the euhedral phenocrysts; they are predominantly lath-shaped to tabular and exhibit low alteration processes, making them clearer than the clinopyroxene. The clinopyroxene crystals appear subhedral, being relatively minor than the plagioclase. During petrographic analysis, it was observed that the more central portions of the profile had a higher proportion of minerals (Figure 6C) compared to the groundmass. In contrast, a greater amount of groundmass was observed in the upper portions (Figure 6A). Furthermore, they exhibit intense alteration via oxidation. Meanwhile, the opaque crystals are euhedral to subhedral and sometimes skeletal (Figure 6C).

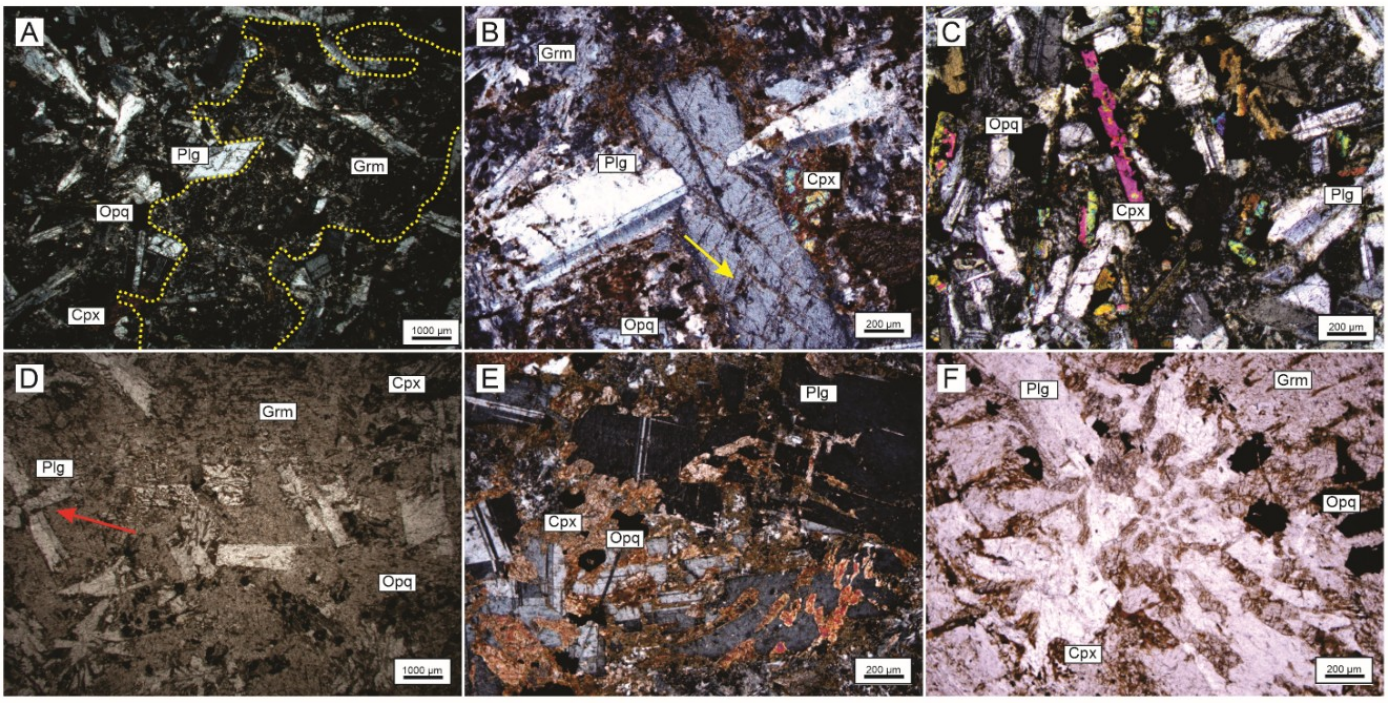

Figure *6*. A. General petrographic aspect of the rock, showing the central mineralogy, under crossed polars. Note the greater development of the cryptocrystalline groundmass (yellow dashed line), forming an intersertal texture. **B.** Sericitization of plagioclase (yellow arrow) and an advanced state of oxidation of clinopyroxene, under crossed polars. **C.** General shape of the rock-forming crystals under crossed polars. **D.** Photomicrograph under plane-polarized light, showing the highly present reddish-brown groundmass, intersertal texture. Note the porphyritic and glomeroporphyritic texture (red arrow). **E.** Intrafascicular texture. **F.** Intrafascicular texture with radial arrangement of clinopyroxenes. Abbreviations: Plg - Plagioclase. Cpx - Clinopyroxene. Opq - Opaque minerals.

The porphyritic and glomeroporphyritic textures predominate, characterized by plagioclase and clinopyroxene phenocrysts immersed in a cryptocrystalline groundmass and intersertal texture (Figure 6D). Moreover, the intrafascicular texture is highlighted here, defined by the intergrowth of clinopyroxene within a plagioclase host crystal (Figure 6E). A radial arrangement of clinopyroxene crystals within plagioclase crystals is also observed in the core of plagioclase, defined by intrafascicular texture (Figure 6F).

4.2. Geochemistry of the Picos-PI Intrusions

For the whole-rock geochemical study, seven samples of hypabyssal intrusive rocks were analyzed. Table 2 presents the nomenclature derived from petrographic analysis, along with the chemical classification and the location of the sample portion within the profile. To enable a comparative study, the geochemical diagrams include representative fields of previously analyzed samples available in the literature, including those from the Sardinha and Mosquito formations, as well as the Pitanga and Paranapanema magma types and the Ceará-Mirim dyke swarms (Fodor et al., 1990; Hollanda et al., 2006; Rocha-Júnior et al., 2013; Heilbron et al., 2018; Oliveira et al., 2018) (Figure 7).

Silica content was selected as the differentiation index for both primary and trace elements, as shown in the Harker diagrams in figures 7 and 8. Nearly all samples exhibit similar geochemical behavior, except one basalt sample (PI-40), which stands out in all bivariate diagrams.

With progressive differentiation, the samples display a slight enrichment trend for K_2O, Na_2O, and P_2O_5. In contrast, negative trends are observed for TiO_2, Al_2O_3, CaO, MgO, and total FeO (Figure 7). Among trace elements, Ba shows a positive correlation with rock evolution, increasing with SiO_2 concentration. At the same time, Sr and Zr exhibit no clear trend (Figure 8).

Given that all samples present high TiO_2 contents (>2.0 wt.%), this oxide was also used as a differentiation index for the same trace elements. In this case, Ba shows an inverse behavior, displaying a negative trend as TiO_2 values increase, whereas Sr and Zr maintain the same pattern, with no apparent trend (Figure 8).

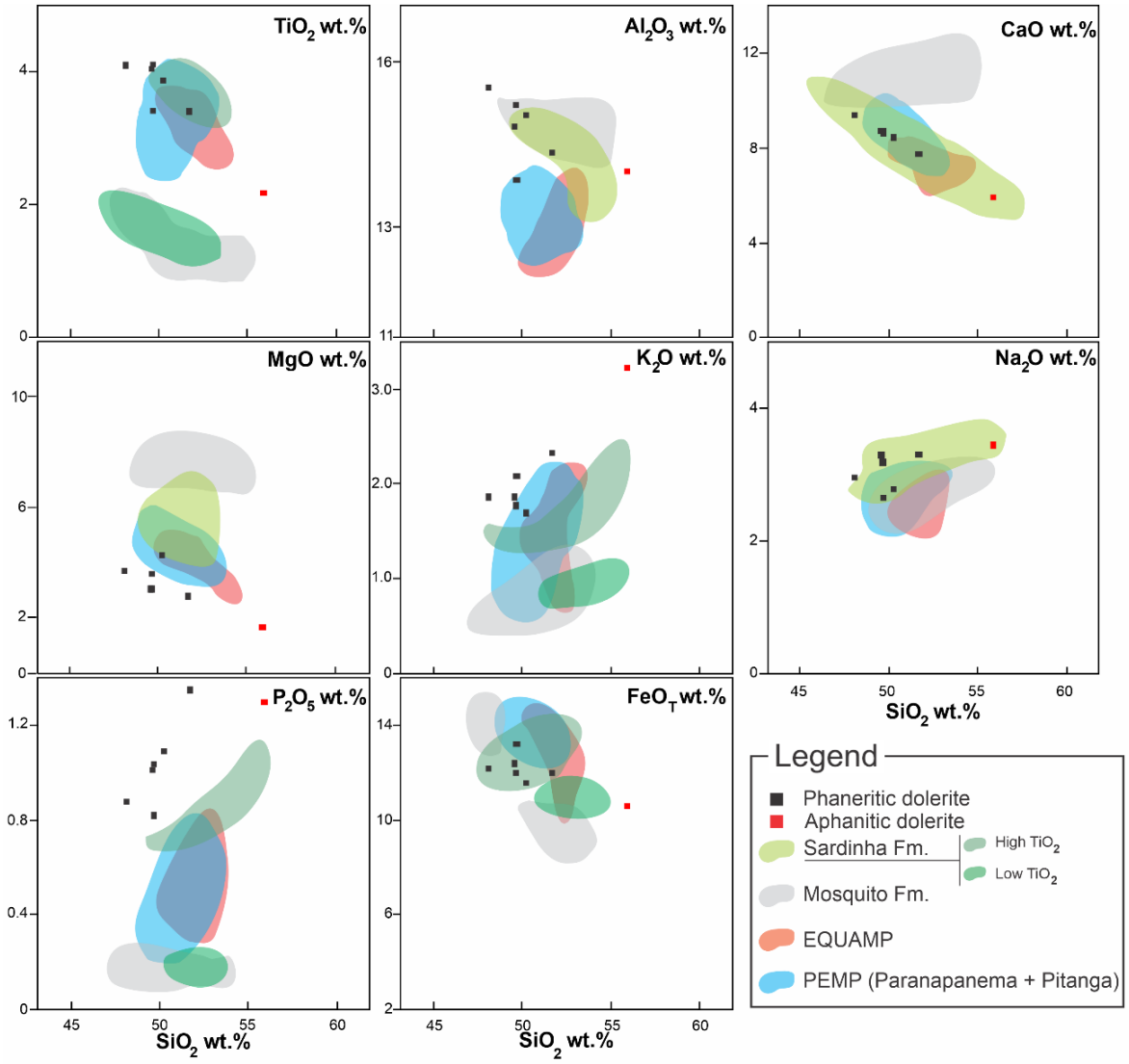

Figure 7. Bivariate diagram for major oxide elements relative to SiO_2.

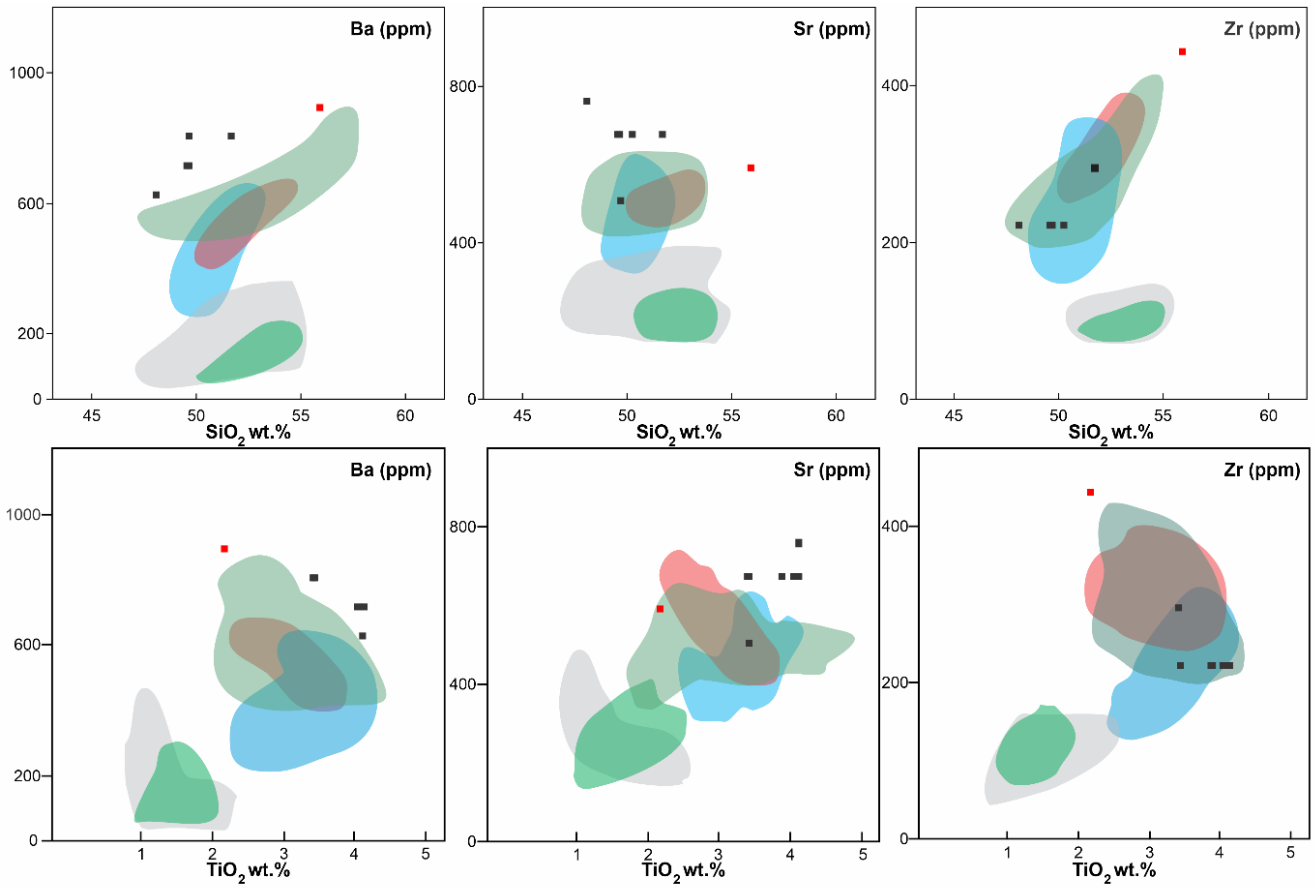

Figure 8. Bivariate diagram for trace elements relative to SiO^2 and TiO^2. Symbol legend as in Figure 7.

Table 2. Geochemical data of whole rock from the igneous intrusions in the Picos region and surrounding areas.

		Samples						
		PI-02	**PI-05A**	**PI-05D**	**PI-07B**	**PI-05C**	**PI-34A**	**PI-40C**
Petrographic classification		Dolerite	Dolerite	Dolerite	Dolerite	Dolerite	Dolerite	Dolerite
Portion of profile		Bottom	Bottom	Top	Core	Core	Bottom	Core
Chemical classification		Basalt	Basalt	Potassic trachybasalt	Basalt	Potassic trachybasalt	Basalt	Latite
Major elements (%)	**SiO_2**	49.68	49.22	49.13	47.68	51.24	49.8	55.91
	TiO_2	3.43	4.09	4.01	4.07	3.38	3.85	2.18
	Al_2O_3	13.86	15.33	14.71	15.39	14.22	14.9	14.02
	Fe_2O_3	14.66	13.21	13.65	13.42	13.25	12.73	11.77
	MnO	-	0.19	0.20	0.17	0.24	0.17	0.18
	MgO	3.60	3.01	3.01	3.68	2.75	4.21	1.67
	CaO	8.61	8.67	8.66	9.30	7.67	8.38	5.92
	Na_2O	2.69	3.16	3.27	2.93	3.27	2.94	3.44
	K_2O	2.09	1.76	1.84	1.85	2.29	1.68	3.23
	P_2O_5	1.04	0.82	1.01	0.87	1.34	1.09	1.31
	LOI	1.75	1.65	1.33	1.33	1.56	2.82	2.67
	SUM	100.61	99.56	99.60	99.47	99.76	99.77	99.76
Trace Elements (ppm)	**Ba**	806	716	716	627	806	-	895
	Sr	507	676	676	761	676	676	592
	Zr	222	222	222	222	296	222	444

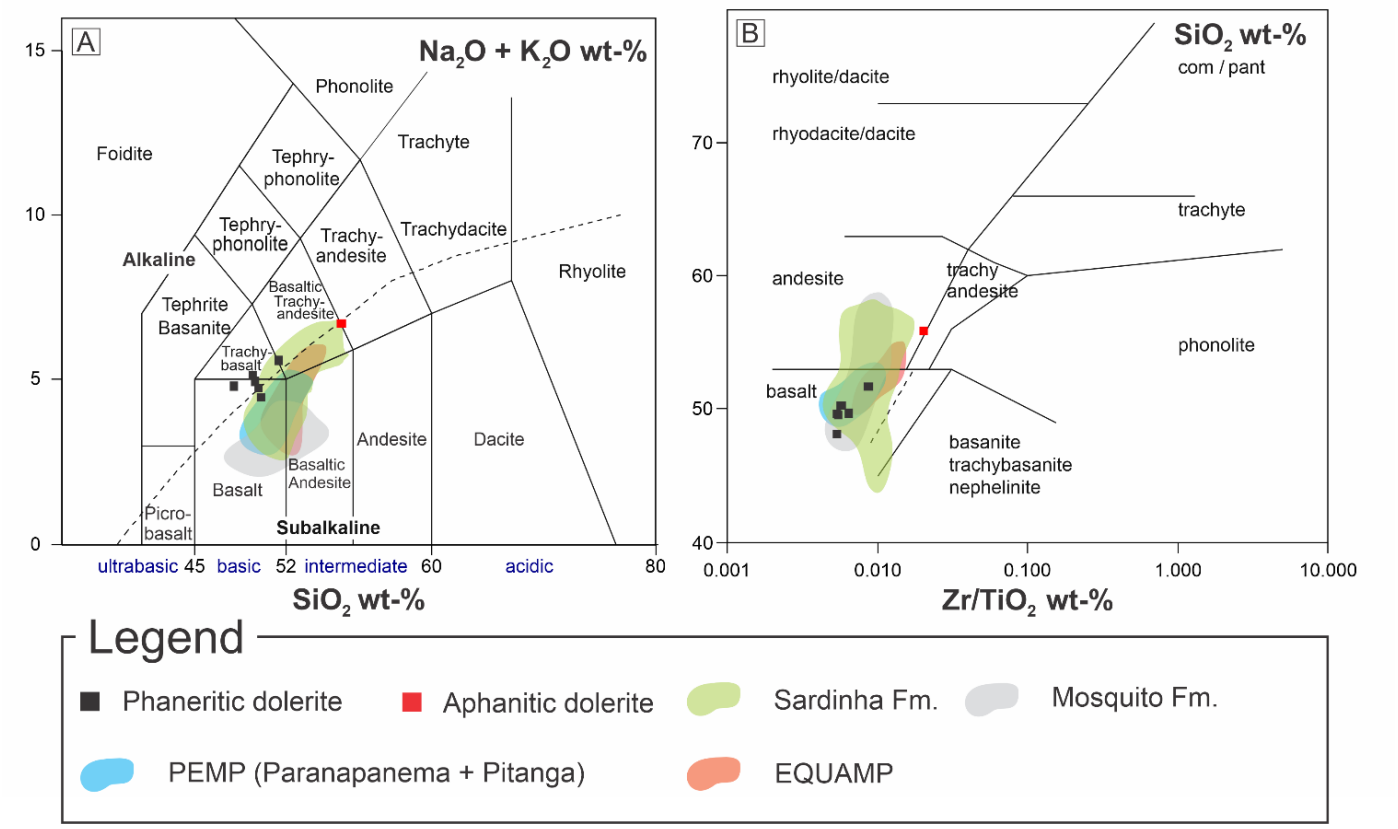

Figure 9. A. Total Alkali vs. Silica diagram. **B.** Diagram SiO_2 vs. Zr/TiO_2. The colored fields represent the compositions of the Sardinha Formation (Fodor et al., 1990; Heilbron et al., 2018; Oliveira et al., 2018). Representing the Central Atlantic Magmatic Province (CAMP) we assump that the Mosquito Formation (Fodor et al., 1990; Oliveira et al., 2018). Central Atlantic Magmatic Province (EQUAMP; Hollanda et al., 2006). Paraná-Etendeka Magmatic Province with Paranapanema and Pitanga magmas type (Rocha-Júnior et al., 2013).

The analyzed samples display a significant variation in SiO_2 (47.04 - 50.44 wt%), MgO (2.71 - 4.09 wt%), CaO (7.55 - 9.18 wt%), Fe_2O_3 (12.37 - 14.41 wt%), and Al_2O_3 (13.61 - 15.18 wt%), with moderate variation in TiO_2 (3.33 - 4.02 wt%), MnO (0.16 - 0.24 wt%), P_2O_5 (0.80 - 1.32 wt%), K_2O (1.63 - 2.26 wt%), and Na_2O (2.64 - 3.22 wt%). The K_2O/Na_2O ratio in these rocks ranges from 0.55 to 0.70. One sample (PI-40C), which is the only one petrographically classified as aphanitic dolerite, stands out for its higher concentrations of SiO_2 (54.41 wt%), Na_2O (3.35 wt%), and K_2O (3.14 wt%), and lower contents of MgO (1.62 wt%), TiO_2 (2.12 wt%), and CaO (5.76 wt%).

All analyzed samples from the Picos region display high TiO_2 concentrations (>2.0 wt.%), according to the criteria proposed by Bellieni et al. (1984) and Mantovani et al. (1985) (Table 2). When plotted on geochemical classification diagrams, these samples overlap with fields corresponding to the Sardinha and Mosquito formations, as well as the PEMP and EQUAMP provinces. However, the Sardinha Formation occupies a broader compositional field, reflecting its wider geochemical variability, which encompasses both high- and low-TiO_2 tholeiitic rocks.

Most of the samples studied plot within the basalt to trachybasalt field, except for sample PI-40C, which falls into the trachyandesite field on the TAS diagram (Figure 9A) (Le Bas et al., 1986). All samples follow an alkaline trend, plotting near the subalkaline series boundary; however, a more subalkaline character is supported by the behavior of immobile trace elements (Figure 9B) (Winchester and Floyd, 1977).

The potassic nature of the samples plotting in the trachybasalt and basaltic trachyandesite fields on the TAS diagram is confirmed by the condition $K_2O > (Na_2O - 2)$. The rocks are accordingly classified as potassic trachybasalt and latite, respectively, following the criteria of Le Maitre et al. (2002).

With respect to magmatic series, all samples exhibit a tholeiitic affinity when plotted on the AFM diagram (Irvine and Baragar, 1971) (Figure 10A). To confirm magmatic evolution along this series, fewer mobile elements were considered in the SiO_2 versus FeO_T/MgO diagram (Miyashiro, 1975), in which all samples also plot within the tholeiitic trend (Figure 10B). Regarding the aluminum saturation index, all samples fall within the metaluminous field in the A/CNK versus A/NK diagram (Shand, 1969) (Figure 10C). According to the magnesium number (#Mg) approach (Murray et al., 2015), all subvolcanic samples from the Picos region display a more evolved geochemical character (Figure 10D).

Regarding tectonic setting classifications, all samples plot within the intraplate field when inserted into the Zr versus Ti diagram (Figure 11A) (Pearce, 1982). This affinity is further supported by the oxide ratios of TiO_2, Al_2O_3, and the trace element Zr, which, when plotted in the

diagrams proposed by Müller et al. (1992), also fall within the intraplate field (figures 11B and 11C).

5. DISCUSSIONS

5.1. Petrographic aspects of the bottom, core, and top sections

The various modes of magma or lava emplacement, combined with their respective cooling and crystallization processes, result in rocks with specific textures that reflect distinct thermal and dynamic regimes (Hulme, 1974; Hastie et al., 2013; Rateau et al., 2013). In this context, effusive rocks, which undergo rapid cooling, typically develop fine-grained to glassy matrices, as well as features such as vesicles, amygdales, and embayment textures (Cox et al., 1979). In contrast, intrusive rocks are associated with slower cooling rates, which favor the development of granular, intergranular, poikilitic, ophitic, and subophitic textures (Cox et al., 1979; Goff, 1996; Le Maitre et al., 2002; Sarmento et al., 2017).

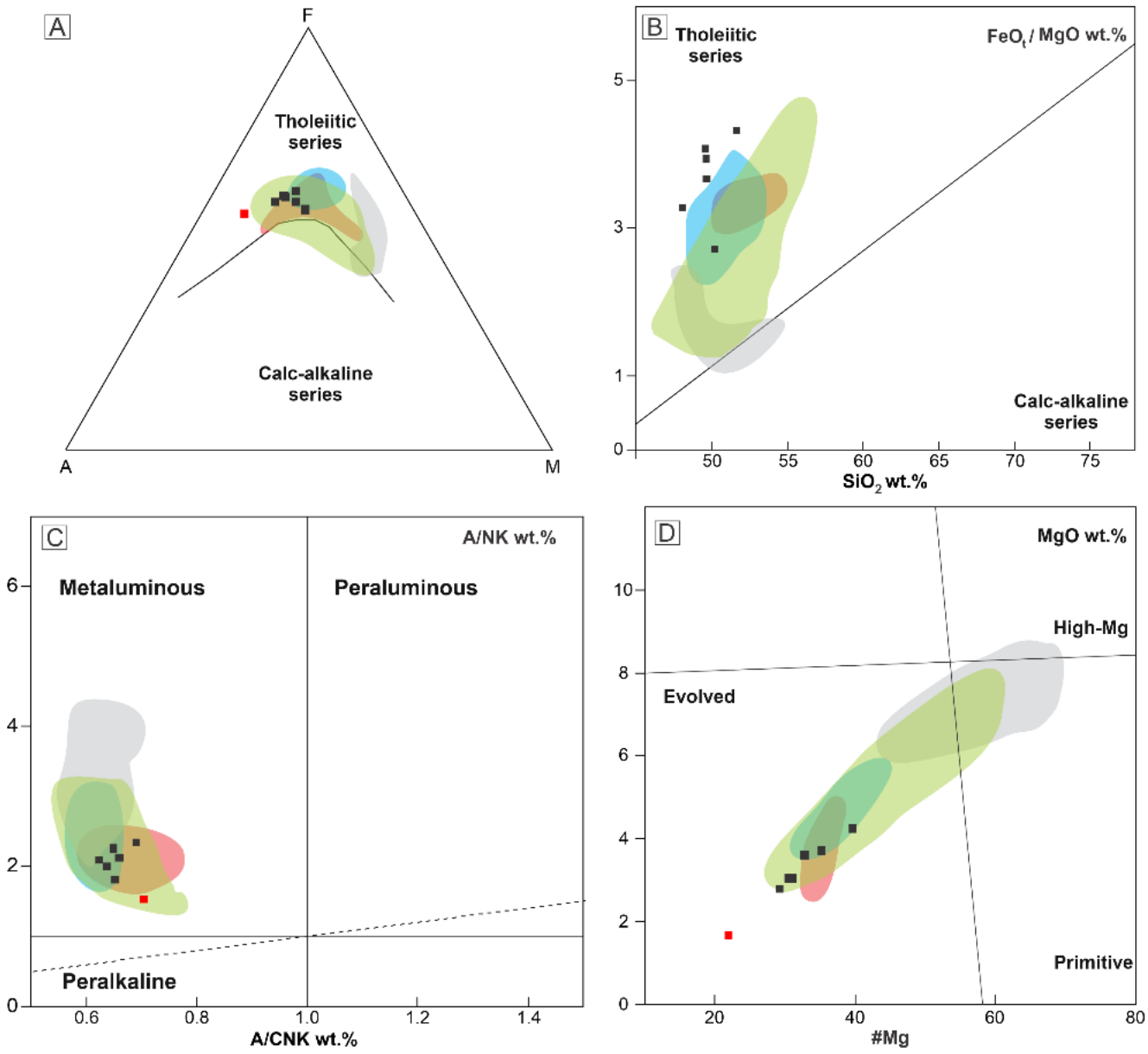

Figure 10. A. Fetotal - CaO - MgO diagram. **B.** FeO_t/MgO vs. SiO_2 ratio diagram. **C.** A/NK vs. A/CNK diagram. **D.** Evolutionary degree diagram MgO vs. #Mg (magnesium number). Symbol legend as in Figure 7.

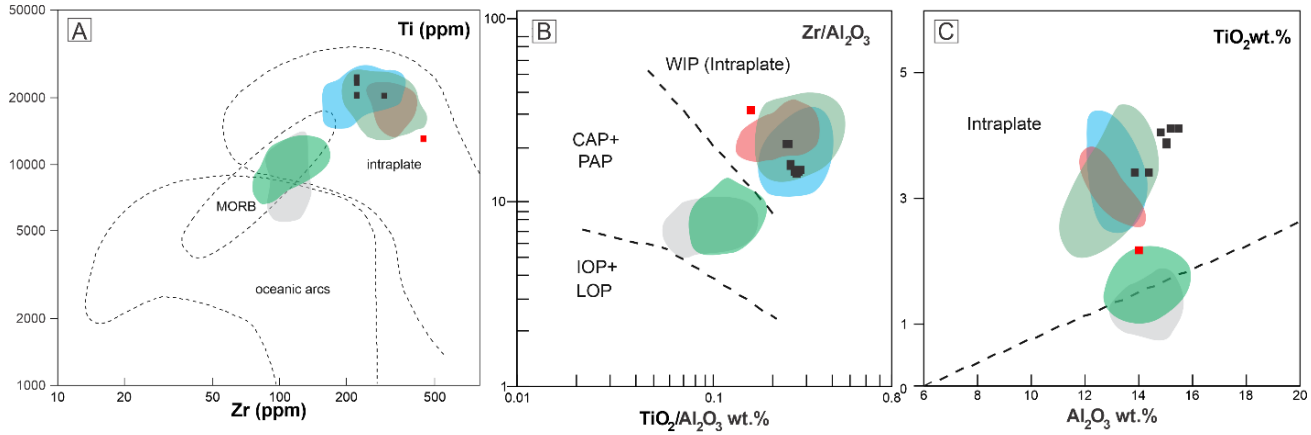

Figure 11. A. Geotectonic classification diagram based on the relationship between Ti vs. Zr. **B.** Classification based on the Zr/Al_2O_3 vs. TiO_2/Al_2O_3 ratio. **C.** Classification based on the TiO_2 vs. Al_2O_3 relationship. Abbreviations: CAP, continental arc potassic rocks; PAP, post-collisional arc potassic rocks Symbol legend as in Figure 7.

Despite this contrast, intersertal, and intrafascicular textures were observed in the cores of aphanitic dolerite (figures 6E and 6F) sills throughout this study. Similarly, previous studies on intrusive rocks of the Sardinha Formation have reported the presence of mesostasis (Baksi and Archibald, 1997; Heilbron et al., 2018; Oliveira et al., 2018). In the aphanitic dolerite sill (Figure 6), a fine-grained groundmass is present in all portions (*Dach* and *Dacv*), accompanied by porphyritic and glomeroporphyritic textures, a radial arrangement of plagioclase crystals, and a predominance of intrafascicular texture in the core. These characteristics were previously observed and described by Silva et al. (2024). It is worth noting that these characteristics, identified in both this study and previous research, are typical of rocks subjected to rapid cooling or those formed near the margins of intrusions.

This strong evidence of faster crystallization in an intrusive environment indicates that the formation mechanism was similar to what has already been observed in other units of the Parnaíba Magmatic Province, such as the Mosquito Formation described by Fornero et al. (2023), which suggests a shallow emplacement of sills based on facies analyses and textural evidence on top, core, and bottom.

The newly described textures in this study are exclusively related to intrusive rocks classified as sills. However, the rapid-crystallization textures observed in the aphanitic dolerite sill (Figure 6) are primarily attributed to a high degree of supersaturation (Drever et al., 1972). This intense supersaturation, which drives rapid nucleation and growth, may have been significantly enhanced by the process of magmatic decompression during emplacement at shallow crustal levels. The ascent and intrusion of the magma into shallower depths promotes volatile exsolution at high rates, a well-established mechanism for increasing supersaturation and generating rapid crystallization textures in shallow intrusions (Drever et al., 1972; Hammer and Rutherford, 2002).

Weedon (1960) described similar textures in aphanitic rocks of the Gars-bheinn intrusion, located in the Cuillins of Skye, southern Scotland. The textures at the top of that intrusion were described as ranging from subophitic to subvariolitic (intrafascicular). In detail, he identified skeletal olivine crystals, occasionally arranged radially, along with epitaxial relationships between plagioclase and pyroxene (Weedon, 1960; Fagan et al., 2013). Later, Drever et al. (1972) used the term intrafascicular texture to describe the intergrowth of pyroxene and plagioclase crystals, with skeletal pyroxene crystals elongated within the cores of plagioclase in lunar rocks. The presence of intrafascicular texture suggests a high degree of supersaturation.

Smith and Lindsley (1971) observed a negative trend for Ca, accompanied by an increase in Fe content, in experimental studies on pyroxene compositions in terrestrial rocks. Similarly, Weill et al. (1971) reported analogous results when analyzing the composition and evolution of pyroxenes with intrafascicular texture. The degree of supersaturation may be interpreted in two stages: the first involves the growth of olivine and pyroxene phenocrysts, as indicated by porphyritic textures, which favor the early crystallization of these minerals. This process results in a relative enrichment in Fe compared to Mg and Ca, especially under shallow conditions (Wyllie, 1963; Bence et al., 1971; Hollister et al., 1971; Drever et al., 1972).

Based on these inferences, a possible model was developed (Figure 12) that explains some of the reasons for the differences in facies and textures observed in the two stratigraphic profiles. Figure 12A shows the intrusion still in the subsurface, followed by erosion that exposes the dolerite sills at the surface (Figure 12B), which are observed as facies in these outcrops, from the base, core, and top. The facies found in the phaneritic dolerite profile

can be explained as portions of the sills: the facies with columnar jointing and matrix, even if isolated, are part of the base and top, while the coarser facies, with the absence of matrix, constitute the core. However, the facies found in the aphanitic dolerites can also explain the finer grain size and the abundant presence of matrix in a more marginal portion of the sill (Figure 12C).

Fornero et al. (2023), although working with data from wells in the Mosquito Formation, arrived at a similar model, albeit with greater detail and differences in facies, such as gabbroic and even pegmatitic facies, which were not seen here. Based on these findings, it can be inferred that the phaneritic dolerite sills (Figure 3) underwent near-equilibrium crystallization, as evidenced by the presence of intergranular (Figure 5G), micrographic texture (Figure 5E). In contrast, the aphanitic dolerite sill indicates a rapid crystallization process involving at least two cooling stages: the first related to the formation of plagioclase phenocrysts, and the second involving the intergrowth of pyroxene and plagioclase, along with groundmass crystallization.

The present study grounds its inferences primarily on the occurrence of porphyritic and intrafascicular textures, using them to support the proposed hypotheses. It is essential to note that, although the consulted literature relies on experimental studies to interpret intrafascicular texture, this work focuses on its petrographic description. Even so, the petrographic results obtained here may contribute to a deeper understanding of the crystallization processes of these sills. They demonstrate that cooling rate and crystallization behavior are not necessarily dependent and further emphasize how physical and chemical factors influence the development of these intrusions.

5.2. Geochemical implications

The origin of the Sardinha Formation remains under discussion, particularly regarding the magmatic event responsible for its genesis. Previous studies have proposed that this formation resulted from magmatic activity related to the Paraná-Etendeka Magmatic Province (PEMP) (Mizusaki and Thomaz Filho, 2004). However, Baksi and Archibald (1997), based on $^{40}Ar/^{39}Ar$ dating of these rocks, suggested that a distinct magmatic event may have generated this unit. Later, Hollanda et al. (2018) proposed a correlation between the Sardinha Formation and a different magmatic episode, designated EQUAMP (Equatorial Atlantic Magmatic Province).

Previous studies have described the volcanic and subvolcanic rocks of the Sardinha Formation as intrusive bodies, primarily represented by dikes and sills, restricted to the eastern portion of the Parnaíba Basin (Sial, 1974; Vaz et al., 2007). Geochemically, the Sardinha Formation has been classified as consisting of basic to intermediate, tholeiitic, metaluminous rocks, with a certain degree of evolution due to fractional crystallization processes (Fodor et al., 1990; Heilbron et al., 2018; Oliveira et al., 2018).

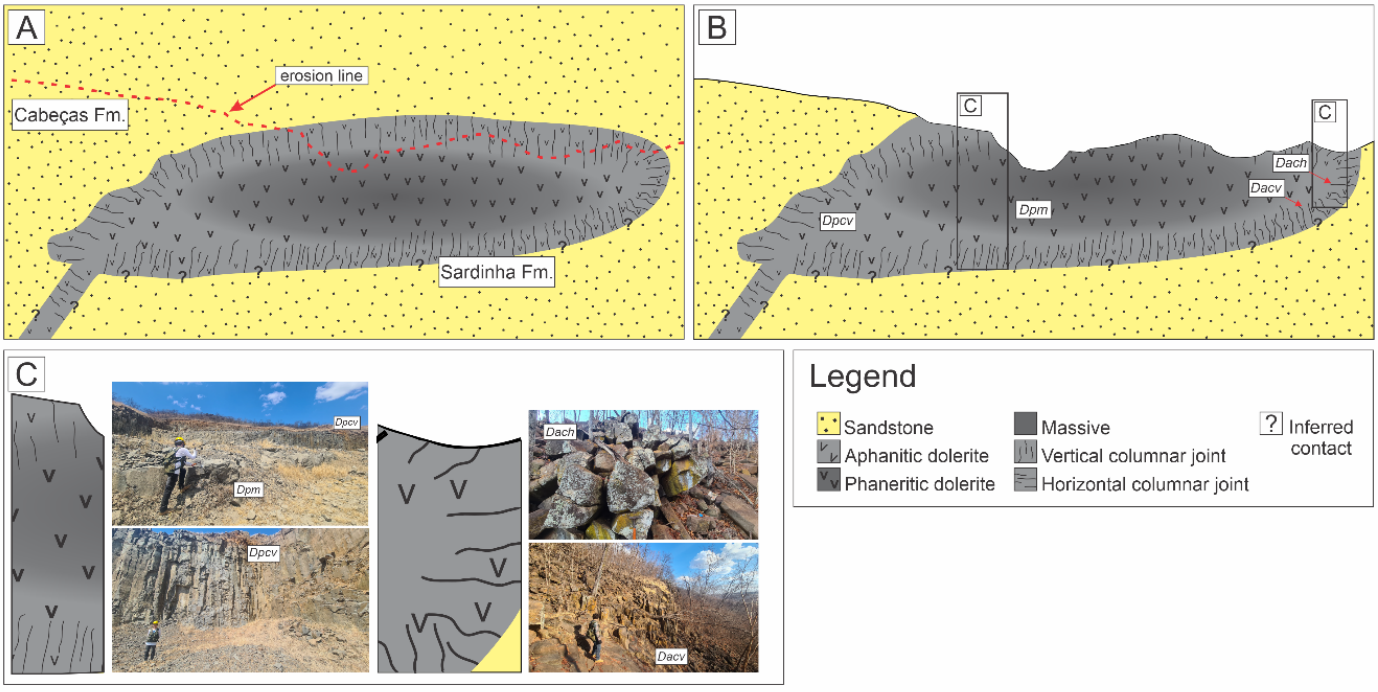

Figure 12. Model of dolerite intrusion. **A.** Possible environment for the sill and host rocks after intrusion. **B.** Exposed outcrop of the sill, showing the different facies of the sill portions. **C.** Integration of the model illustration with the facies observed in the field.

The present study conducted in the Picos region (Piauí) enabled the geochemical classification of the sampled basic rocks as basalts, trachybasalts, and trachyandesite, including an aphanitic basalt (Figure 6C). These samples exhibit tholeiitic affinity (Figure 7), metaluminous character (Figure 7), and evidence of geochemical evolution (Figure 7). Furthermore, the samples plot within the intraplate tectonic field (Figure 11), which may be attributed to crustal assimilation during intrusion processes a possibility supported by the high TiO_2 content, which will be discussed further.

With regard to magmatic differentiation, a negative correlation between MgO and SiO_2 (Figure 7) was observed, consistent with fractional crystallization driven by the removal of mafic minerals from the system (Bowen, 1928). A decrease in Al_2O_3, associated with CaO depletion, likely reflects the crystallization of plagioclase.

The decrease in total FeO is not common in tholeiitic magmas; indeed, the crystallization of magmas begins with an increase, as the Fenner trend, following an inflection point and a decrease in the final stages (Fenner, 1929). As seen in Figure 7, the decrease in iron content may be attributed to the inflection point or final stages of crystallization of oxide minerals, resulting from the crystallization of iron oxide minerals such as magnetite and ilmenite at low temperatures (Walker 1930; Fenner, 1931).

Additionally, a progressive increase followed by a decline in P_2O_5 content suggests the onset of apatite crystallization the principal accessory mineral identified in these rocks. Alkali contents, however, did not exhibit consistent trends.

Nonetheless, the geochemical variability of the Sardinha Formation poses a challenge for correlation using major element geochemistry alone. The studied samples fall within the broader compositional field of this formation in several diagrams (figures. 7 to 11). In contrast, the compositional fields associated with the Mosquito Formation (CAMP), PEMP, and EQUAMP are more limited and occasionally overlap with Sardinha. Another complicating factor is the absence of trace element and rare earth element data in the present study, which limits the ability to distinguish more precisely among these magmatic provinces, particularly between the Paraná-Etendeka and Equatorial Atlantic systems.

Despite these limitations, the studied samples consistently exhibit a geochemical behavior that closely matches that of the Sardinha Formation, particularly its high-TiO_2 subgroup (Figure 8). This geochemical affinity reinforces the petrographic evidence presented earlier in this work, which aligns with descriptions found in the literature for the Sardinha Formation (Fodor et al., 1990; Heilbron et al., 2018; Oliveira et al., 2018).

Still, the observed variability within the Sardinha Formation supports the need for a more detailed subdivision into distinct magma types, as suggested by Oliveira et al. (2018). Additionally, absolute geochronological analyses of these rocks would be of great significance for distinguishing among the various magmatic events that affected the Parnaíba Basin.

This study contributes to the expansion of available geochemical data for these rocks, providing a foundation for future investigations. The data presented here may serve as a reference for subsequent studies aiming to deepen our understanding of the Sardinha Formation and its magmatic evolution.

6. CONCLUSIONS

The present study, conducted on basic sills from the Picos region (Piauí), located in the eastern sector of the Parnaíba Basin, provided a pioneering lithofacies classification of intrusive rocks, along with detailed petrographic descriptions of their basal, core, and upper sections, supported by major and minor element geochemistry. The contrasting textures observed in the phaneritic, and aphanitic dolerite sills allowed for the interpretation of differing crystallization rates. The petrography of the phaneritic dolerite indicates a slower, equilibrium-controlled cooling and crystallization regime, whereas the aphanitic sill presents evidence of more rapid crystallization, particularly through the occurrence of intrafascicular texture and abundance of groundmass in comparison with phaneritic dolerite.

Considering the spatial distribution, of these intrusive rocks within the eastern sector of the basin, an area traditionally regarded as hosting occurrences of the Sardinha Formation and the petrographic similarities between the studied dolerite sills and those previously described in the literature, it is concluded that the analyzed samples belong to the Sardinha Formation. Moreover, the geochemical characteristics of the samples indicate affinity with the high-TiO_2 subgroup of this formation. Thus, this work concludes that the basic sills in the Picos region are part of the broader geochemical unit known as the Sardinha Formation.

However, the compilation of geochemical data from multiple studies reveals a wide range of chemical characteristics for the Sardinha Formation, in contrast to the more restricted and provincial signature of the Mosquito Formation. Therefore, further studies aimed at subdividing the Sardinha Formation into distinct magmatic subtypes are necessary. Such investigations would facilitate a more refined understanding of the emplacement processes and magmatic evolution of this important geological unit.

ACKNOWLEDGMENTS

I extend my sincere gratitude to the PRH 47.1 Program, coordinated by Professor Mário Lima Filho, whose support and the undergraduate scholarship granted by the program were essential for the completion of this work. I also acknowledge Neg-Labise/UFPE for performing the geochemical analyses. My appreciation is likewise directed to the VULCANO and Geoquantt research groups and laboratories for the valuable support provided throughout this study.

REFERENCES

Abrantes Júnior, F.R., and Nogueira, A.C.R., 2013, Reconstituição paleoambiental das formações Motuca e Sambaíba, Permo-Triássico da Bacia do Parnaíba no sudoeste do Estado do Maranhão, Brasil: Geologia USP, Série Científica, v. 13, n. 3, p. 65-82, doi: https://doi.org/10.5327/Z1519-874X201300030007.

Almeida, F.F.M., and Carneiro, C.D.R., 2004, Inundações marinhas fanerozóicas no Brasil e recursos minerais associados, *in* Mantesso Neto, V., Bartorelli, A., Carneiro, C.D.R. and Brito-Neves, B.B., 2004: Geologia do Continente Sul-Americano: Evolução da obra de Fernando Flávio Marques de Almeida: Beca: São Paulo, p. 43-58.

Angelim, L.A.A., Vasconcelos, A.M., Gomes, J.R.C., Wanderley, A.A., Forgiarini, L.L., and Medeiros, M.F., 2004, Folha SB.24-Jaguaribe, *in* Schobbenhaus, C., Gonçalves, J.H., Santos, J.O.S., Abram, M.B., Leão Neto, R., Matos, G.M.M., Vidotti, R.M., Ramos, M.A.B., e Jesus, J.D.A., eds., Carta Geológica do Brasil ao Milionésimo, Sistema de Informações Geográficas (SIG): Programa Geologia do Brasil, CPRM - Serviço Geológico do Brasil, Brasília, CD-ROM.

Arai, M., 2014, Aptian/Albian (Early Cretaceous) paleogeography of the South Atlantic: a paleontological perspective: Brazilian Journal of Geology, v. 44, n. 2, p. 339-350, doi: https://doi.org/10.5327/Z2317-4889201400020012.

Baksi, A.K., and Archibald, D.A., 1997, Mesozoic igneous activity in the Maranhão province, northern Brazil: $^{40}Ar/^{39}Ar$ evidence for separate episodes of basaltic magmatism: Earth and Planetary Science Letters, v. 151, n. 3-4, p. 139-153, doi: https://doi.org/10.1016/S0012-821X(97)81844-4.

Barreto, C.J.S., Lima, E.F., Scherer, C.M., and Rossetti, L.D.M.M., 2014, Lithofacies analysis of basic lava flows of the Paraná igneous province in the south hinge of Torres Syncline, Southern Brazil: Journal of Volcanology and Geothermal Research, v. 285, p. 81-99, doi: https://doi.org/10.1016/j.jvolgeores.2014.08.008.

Bellieni, G., Comin-Chiaramonti, P., Marques, L.S., Melfi, A.J., Piccirillo, A.J.R., and Roisemberg, A., 1984, High-and-low-TiO2 flood basalts from the Paraná Plateau (Brazil): petrology and geochemical aspects bearing on their mantle origin: Stuttgart: Neues Jahrbuch fur Mineralogie, v. 150, n. 3, p. 273-306.

Bellieni, G., Piccirillo, E.M., Cavazzini, G., Petrini, R., Comin Chiaramonti, P., Nardy, A.J.R., and Zantedeschi, P., 1990, Low-TiO2 and high-TiO2 Mesozoic tholeiitic magmatism of the Maranhão basin (NE-Brazil): K/Ar age, geochemistry, petrology, isotope characteristics and relationships with Mesozoic low-TiO2 and high-TiO2 flood basalts of the Paraná basin (SE Brazil): Neues Jahrbuch für Mineralogie Abhandlungen, v. 162, p. 1-33.

Bence, A.E., Papike, J.J., and Lindsley, D.H., 1971, Crystallization histories of clinopyroxenes in two porphyritic rocks from Oceanus Procellarum, *in* Proceedings of the Lunar Science Conference: Cambridge, The MIT Press, v. 2, p. 559.

Bowen, N.L., 1928, The evolution of the igneous rocks: Princeton, Princeton University Press, 332 p.

Caputo, M.V., 1985, Late Devonian glaciation in South America: Palaeogeography, Palaeoclimatology, Palaeoecology, v. 51, n. 1-4, p. 291-317, doi: https://doi.org/10.1016/0031-0182(85)90090-2.

Cas, R.A.F., and Wright, J.V., 1987, Volcanic successions-modern and ancient: A geological approach to processes, products and successions: London: ALLEN and Unwin, 529 p.

Cioccari, G.M., and Mizusaki, A.M.P., 2019, Sistemas petrolíferos atípicos nas bacias paleozoicas brasileiras - uma revisão: Geociências, v. 38, n. 2, p. 367-390, doi: https://doi.org/10.5016/geociencias.v38i2.13173.

Coffin, M.F., and Eldholm, O., 1992, Volcanism and continental break-up: a global compilation of large igneous provinces: Geological Society, London, Special Publications, v. 68, n. 1, p. 17-30, doi: https://doi.org/10.1144/gsl.sp.1992.068.01.02.

Coffin, M.F., and Eldholm, O., 1994, Large igneous provinces: Crustal structure, dimensions, and external consequences: Reviews of Geophysics, v. 32, n. 1, p. 1-36, doi: https://doi.org/10.1029/93rg02508.

Coffin, M.F., and Eldholm, O., 2001, Large igneous provinces: Progenitors of some ophiolites?, in Mantle plumes: their identification through time: Geological Society of America, doi: https://doi.org/10.1130/0-8137-2352-3.59.

Cox, K.G., Bell, J.D., and Pankhurst, R.J., 1979, The interpretation of igneous rocks: Dordrecht, Springer Netherlands, doi: https://doi.org/10.1007/978-94-017-3373-1.

Drever, H.I., Johnston, R., Butler Jr, P., and Gibb, F.G.F., 1972, Some textures in Apollo 12 lunar igneous rocks and in terrestrial analogs, *in* Proceedings of the Lunar Science Conference: Cambridge, Mass., M.I.T. Press, v. 3, p. 171.

Ernesto, M., Bellieni, G., Piccirillo, E.M., Marques, L.S., Min, A., Pacca, I.G., Martins, G., and Macedo, J.W. P., 2003, Paleomagnetic and geochemical constraints on the timing and duration of the CAMP activity in northeastern Brazil, *in* The Central Atlantic Magmatic Province: Insights From Fragments of Pangea: Washington, D. C., American Geophysical Union, p. 129-149, doi: https://doi.org/10.1029/136gm07.

Ewart, A., 2004, Petrology and geochemistry of early cretaceous bimodal continental flood volcanism of the NW Etendeka, Namibia. Part 1: Introduction, mafic lavas and re-evaluation of mantle source components: Journal of Petrology, v. 45, n. 1, p. 59-105, doi: https://doi.org/10.1093/petrology/egg083.

Fagan, A.L., Neal, C.R., Simonetti, A., Donohue, P.H., and O'Sullivan, K.M., 2013, Distinguishing between Apollo 14 impact melt and pristine mare basalt samples by geochemical and textural analyses of olivine: Geochimica et Cosmochimica Acta, v. 106, p. 429-445, doi: https://doi.org/10.1016/j.gca.2012.12.032.

Fenner, C.N., 1929, The crystallization of basalts: American Journal of Science, v. 18, n. 105, p. 225-253.

Fenner, C.N., 1931, The residual liquids of crystallizing magmas: Mineralogical magazine and journal of the Mineralogical Society, v. 22, n. 134, p. 539-560, doi: https://doi.org/10.1180/minmag.1931.022.134.01.

Fodor, R.V., Sial, A.N., Mukasa, S.B., and McKee, E.H., 1990, Petrology, isotope characteristics, and K-Ar ages of the Maranhão, northern Brazil, Mesozoic basalt province: Contributions to Mineralogy and Petrology, v. 104, n. 5, p. 555-567, doi: https://doi.org/10.1007/bf00306664.

Fornero, S.A., Millett, J.M., Lima, E.F., Jesus, C.M., Bevilaqua, L.A., and Marins, G.M., 2023, Emplacement dynamics of a complex thick mafic intrusion revealed by borehole image log facies analyses: Implications for fluid migration in the Parnaíba Basin petroleum system, Brazil: Marine and Petroleum Geology, v. 155, doi: https://doi.org/10.1016/j.marpetgeo.2023.106378.

Góes, A.M., and Feijó, F.J., 1994, Bacia do Parnaíba: Boletim de Geociências da Petrobras, v. 8, no. 1, p. 57-67, https://bgp.petrobras.com.br/bgp/article/view/581 (accessed August 2025).

Goff, F., 1996, Vesicle cylinders in vapor-differentiated basalt flows: Journal of Volcanology and Geothermal Research, v. 71, n. 2-4, p. 167-185, doi: https://doi.org/10.1016/0377-0273(95)00073-9.

Hames, W.E., Renne, P.R., and Ruppel, C., 2000, New evidence for geologically instantaneous emplacement of earliest Jurassic Central Atlantic magmatic province basalts on the North American margin: Geology, v. 28, n. 9, p. 859-862, doi: https://doi.org/10.1130/0091-7613(2000)028%3C0859:nefgie%3E2.3.co;2.

Hames, W.E., McHone, J.G., Renne, P., and Ruppel, C., 2003, Introduction, in The Central Atlantic Magmatic Province: insights from fragments of Pangea: Washington, D. C., American Geophysical Union, p. 1-6, doi: https://doi.org/10.1029/136gm01.

Hammer, J.E., and Rutherford, M.J. (2002). An experimental study of the kinetics of decompression-induced crystallization in silicic melt: Journal of Geophysical Research: Solid Earth, v. 107, n. B1, p. ECV 8-1-ECV 8-24, doi: https://doi.org/10.1029/2001JB000281.

Hastie, W.W., Watkeys, M.K., and Aubourg, C., 2013, Characterisation of grain-size, shape and orientation of plagioclase in the Rooi Rand dyke swarm, South Africa: Tectonophysics, v. 583, p. 145-157, doi: https://doi.org/10.1016/j.tecto.2012.10.035.

Heilbron, M., Guedes, E., Mane, M., Valeriano, C.M., Tupinambá, M., Almeida, J., Silva, L.G.E., Duarte, B.P., Favera, J.C.D., and Viana, A., 2018, Geochemical and temporal provinciality of the magmatism of the eastern Parnaíba Basin, NE Brazil: Geological Society, London, Special Publications, v. 472, n. 1, p. 251-278, doi: https://doi.org/10.1144/sp472.11.

Hollanda, M.H.B.M., Pimentel, M.M., Oliveira, D.C., and de Sá, E.F.J., 2006, Lithosphere - asthenosphere interaction and the origin of Cretaceous tholeiitic magmatism in Northeastern Brazil: Sr - Nd - Pb isotopic evidence: Lithos, v. 86, n. 1-2, p. 34-49, doi: https://doi.org/10.1016/j.lithos.2005.04.004.

Hollanda, M.H.B.M., Archanjo, C.J., Macêdo Filho, A.A., Fossen, H., Ernst, R.E., Castro, D.L., Melo, A.C., and Oliveira, A.L., 2018, The Mesozoic Equatorial Atlantic Magmatic Province (EQUAMP): A new Large Igneous Province in South America, in Springer Geology: Singapore, Springer Singapore, p. 87-110, doi: lhttps://doi.org/10.1007/978-981-13-1666-1_3.

Hollister, L.S., Trzcienski Jr, W.E., Hargraves, R.B., and Kulick, C.G., 1971, Petrogenetic significance of pyroxenes in two Apollo 12 samples, *in* Proceedings of the Lunar Science Conference, v. 2, p. 529.

Hulme, G., 1974, The interpretation of lava flow morphology: Geophysical Journal International, v. 39, n. 2, p. 361-383, doi: https://doi.org/10.1111/j.1365-246x.1974.tb05460.x.

Irvine, T.N., and Baragar, W.R.A.F., 1971, A guide to the chemical classification of the common volcanic rocks: Canadian journal of earth sciences, v. 8, n. 5, p. 523-548.

Janoušek, V., Farrow, C. M., and Erban, V., 2006, Interpretation of whole-rock geochemical data in igneous geochemistry: introducing Geochemical Data Toolkit (GCDkit): Journal of Petrology, v. 47, n. 6, p. 1255-1259, doi: 10.1093/petrology/egl013.

Jerram, D.A., 2002, Volcanology and facies architecture of flood basalts, in Volcanic Rifted Margins: Geological Society of America, doi: https://doi.org/10.1130/0-8137-2362-0.119.

Le Bas, M.J., Maitre, R.W.L., Streckeisen, A., and Zanettin, B., 1986, A chemical classification of volcanic rocks based on the Total Alkali-Silica Diagram: Journal of Petrology, v. 27, n. 3, p. 745-750, doi: https://doi.org/10.1093/petrology/27.3.745.

Le Maitre, R.W., Streckeisen, A., Zanettin, B., Le Bas, M.J., Bonin, B., Bateman, P., and Woolley, A.R., 2002, Igneous Rocks: a classification and glossary of terms: recommendations of the International Union of Geological Sciences Subcommission on the Systematics of Igneous Rocks: Cambridge, UK, Cambridge University Press, p. 252, doi: https://doi.org/10.1017/CBO9780511535581.

Macêdo Filho, A.A., and Hollanda, M.H.B.M., 2022, Petrogenesis of Mesozoic giant dike swarms and geodynamical insights about EMI-Gough flavors in the Equatorial Atlantic Magmatic Province: Lithos, v. 412-413, doi: https://doi.org/10.1016/j.lithos.2022.106611.

Macêdo Filho, A.A., Hollanda, M.H.B.M., Fraser, S., Oliveira, A.L., Melo, A.C., and Dantas, A., 2023, Correlations among large igneous provinces related to the West Gondwana breakup: A geochemical database reappraisal of Early Cretaceous plumbing systems: Geoscience Frontiers, v. 14, n. 1, doi: https://doi.org/10.1016/j.gsf.2022.101479.

Mantovani, M.S.M., Marques, L.S., De Sousa, M.A., Civetta, L., Atalla, L., and Innocenti, F., 1985, Trace element and strontium isotope constraints on the origin and evolution of Paraná Continental Flood Basalts of Santa Catarina State (Southern Brazil): Journal of Petrology, v. 26, n. 1, p. 187-209, doi: https://doi.org/10.1093/petrology/26.1.187.

Marzoli, A., Renne, P.R., Piccirillo, E.M., Ernesto, M., Bellieni, G., and Min, A.D, 1999, Extensive 200-million-year-old continental flood basalts of the Central Atlantic Magmatic Province: Science, v. 284, n. 5414, p. 616-618, doi: https://doi.org/10.1126/science.284.5414.616.

McPhie, J., 1993, Volcanic textures: A guide to the interpretation of textures in volcanic rocks. Hobart, Tasmania: Centre for Ore Deposit and Exploration Studies, University of Tasmania, p. 198.

Milani, E.J., and Zalán, P.V., 1999, An outline of the geology and petroleum systems of the Paleozoic interior basins of South America: Episodes, v. 22, n. 3, p. 199-205, doi: https://doi.org/10.18814/epiiugs/1999/v22i3/007.

Miranda, F.D, 2014, Pimenteiras Shale: Characterization of an atypical unconventional petroleum system, Parnaíba Basin, Brazil, *in* AAPG International Conference & Exhibition, p. 22.

Miyashiro, A., 1975, Volcanic rock series and tectonic setting: Annual Review of Earth and Planetary Sciences, v. 3, n. 1, p. 251-269, doi: https://doi.org/10.1146/annurev.ea.03.050175.001343.

Mizusaki, A.M.P., Thomaz Filho, A., Milani, E.J., and Césero, P., 2002, Mesozoic and Cenozoic igneous activity and its tectonic control in northeastern Brazil: Journal of South American Earth Sciences, v. 15, n. 2, p. 183-198, doi: https://doi.org/10.1016/s0895-9811(02)00014-7.

Mizusaki, A.M.P., and Thomaz Filho, A., 2004, O magmatismo pós-paleozóico no Brasil, in Mantesso Neto, V., Bartorelli, A., Carneiro, C. D. R. e Brito-Neves, B. B., 2004: Geologia do Continente Sul-Americano: Evolução da obra de Fernando Flávio Marques de Almeida: Beca: São Paulo, p. 281-291.

Müller, D., Rock, N.M.S., and Groves, D.I., 1992, Geochemical discrimination between shoshonitic and potassic volcanic rocks in different tectonic settings: A pilot study: Mineralogy and Petrology, v. 46, n. 4, p. 259-289, doi: https://doi.org/10.1007/bf01173568.

Murray, K.E., Ducea, M.N., and Schoenbohm, L., 2015, Foundering-driven lithospheric melting: The source of central Andean mafic lavas on the Puna Plateau (22°S - 27°S), In: Murray, K. E.; Ducea, M. N.; Schoenbohm, L., Geodynamics of a Cordilleran Orogenic System: The Central Andes of Argentina and Northern Chile: Geological Society of America, 2015, doi: https://doi.org/10.1130/2015.1212(08).

Oliveira, A.L., Pimentel, M.M., Fuck, R.A., and Oliveira, D.C., 2018, Petrology of Jurassic and Cretaceous basaltic formations from the Parnaíba Basin, NE Brazil: correlations and associations with large igneous provinces: Geological Society, Special Publications, v. 472, n. 1, p. 279-308, doi: https://doi.org/10.1144/sp472.21.

Pearce, J.A., 1982, Trace element characteristics of lavas from destructive plate boundaries, *in* Thorpe, R.S., ed., Orogenic Andesites and Related Rocks: Chichester, UK, John Wiley & Sons, p. 525-548.

Pereira, E., Carneiro, C.D.R., Bergamaschi, S., and Almeida, F.D., 2012, Evolução das sinéclises paleozoicas: províncias Solimões, Amazonas, Parnaíba e Paraná, *in* Hasui, Y., Carneiro, C.D.R., de Almeida, F.F.M., and Bartorelli, A., eds., Geologia do Brasil: São Paulo, Beca, p. 374-394.

Rateau, R., Schofield, N., and Smith, M., 2013, The potential role of igneous intrusions on hydrocarbon migration, West of Shetland: Petroleum Geoscience, v. 19, n. 3, p. 259-272, doi: https://doi.org/10.1144/petgeo2012-035.

Rämö, O.T., Heikkilä, P.A., and Pulkkinen, A.H., 2016, Geochemistry of Paraná-Etendeka basalts from Misiones, Argentina: Some new insights into the petrogenesis of high-Ti continental flood basalts: Journal of South American Earth Sciences, v. 67, p. 25-39, doi: https://doi.org/10.1016/j.jsames.2016.01.008.

Rezende, G.L., Martins, C.M., Nogueira, A.C., Domingos, F.G., and Ribeiro-Filho, N., 2021, Evidence for the Central Atlantic magmatic province (CAMP) in Precambrian and Phanerozoic sedimentary basins of the southern Amazonian Craton, Brazil: Journal of South American Earth Sciences, v. 108, doi: https://doi.org/10.1016/j.jsames.2021.103216.

Rocha-Júnior, E.R.V., Marques, L.S., Babinski, M., Nardy, A.J. R., Figueiredo, A.M.G., and Machado, F.B., 2013, Sr - Nd - Pb isotopic constraints on the nature of the mantle sources involved in the genesis of the high-Ti tholeiites from northern Paraná Continental Flood Basalts (Brazil): Journal of South American Earth Sciences, v. 46, p. 9-25, doi: https://doi.org/10.1016/j.jsames.2013.04.004.

Rossetti, L.M., Lima, E.F., Waichel, B.L., Scherer, C.M., and Barreto, C.J., 2014, Stratigraphical framework of basaltic lavas in Torres Syncline main valley, southern Parana-Etendeka Volcanic Province: Journal of South American Earth Sciences, v. 56, p. 409-421, doi: https://doi.org/10.1016/j.jsames.2014.09.025.

Sarmento, C.C.T., Sommer, C.A., and Lima, E.F., 2017, Mafic subvolcanic intrusions and their petrologic relation with the volcanism in the south hinge Torres Syncline, Paraná-Etendeka Igneous Province, southern Brazil: Journal of South American Earth Sciences, v. 77, p. 70-91, doi: https://doi.org/10.1016/j.jsames.2017.04.017.

Shand, 1969, The eruptive Rocks: Hafner Publishing, 488 p.

Sial, A.N., 1974, Petrology and Tectonic significance of the Post-Paleozoic Basaltic rocks of Northeast Brazil.: California, Davis: University of California, 403 p.

Silva, F.M.R., Barreto, C.J.S., Costa, S.G., and Alves, J.V.A., 2024, Análise faciológica e morfológica das rochas hipabissais da região de Picos (PI), porção leste da Bacia Parnaíba: Estudos Geológicos, v. 34, n. 1, p. 1-22, doi: https://doi.org/10.51359/1980-8208.2024.264641.

Smith, D., and Lindsley, D.H., 1971, Stable and metastable augite crystallization trends in a single basalt flow: American Mineralogist, v. 56, p. 225-233.

Thomaz Filho, A., Mizusaki, A.M.P., Milani, E.J., and Cesero, P.D., 2000, Rifting and magmatism associated with the South America and Africa break up: Revista Brasileira de Geociências, v. 30, n. 1, p. 017-019, doi: https://doi.org/10.25249/0375-7536.2000301017019.

Vaz, P.T., Rezende, N.G.A.M., Wanderley Filho, J.R., and Travassos, W.A.S., 2007, Bacia do Parnaíba: Boletim de Geociências da Petrobras, v. 15, p. 253-263, https://bgp.petrobras.com.br/bgp/article/view/308 (accessed August 2025).

Walker, F., 1930, A tholeiitic phase of the quartz-dolerite magma of central Scotland: Mineralogical magazine and journal of the Mineralogical Society, v. 22, n. 130, p. 368-376, doi: https://doi.org/10.1180/minmag.1930.22.130.02.

Waichel, B.L., Wormsbecker, B.T., Lima, E.F., Carmo, I.O., Del Mouro, L., Koester, E., and Kuchle, J., 2024, Exploring the formation of Tangará Sill: A single-pulse intrusion feeding CAMP lava flows in Parecis Basin, Brazil: Journal of South American Earth Sciences, v. 141, doi: https://doi.org/10.1016/j.jsames.2024.104921.

Weedon, D.S., 1960, The Gars-Bheinn Ultrabasic Sill, Isle Of Skye: Quarterly Journal of the Geological Society, v. 116, n. 1-4, p. 37-54, doi: https://doi.org/10.1144/gsjgs.116.1.0037.

Weill, D.F., Grieve, R.A., McCallum, I.S., and Bottinga, Y., 1971, Mineralogy-petrology of lunar samples Microprobe studies of samples 12021 and 12022; viscosity of melts of selected lunar compositions, *in* Proceedings of the Second Lunar Science Conference, v. 1: Cambridge, Massachusetts, The M.I.T. Press, p. 413-430.

Winchester, J.A., and Floyd, P.A., 1977, Geochemical discrimination of different magma series and their differentiation products using immobile elements: Chemical Geology, v. 20, p. 325-343, doi: https://doi.org/10.1016/0009-2541(77)90057-2.

Wyllie, P.J., 1963, Effects of the changes in slope occurring on liquidus and solidus paths in the system diopside-anorthite-albite: Mineralogical Society of America Special Paper 1, p. 204-212.

Zalán, P. V., 2004, Evolução fanerozóica das bacias sedimentares brasileiras, *in* Mantesso Neto, V., Bartorelli, A., Carneiro, C.D.R. and Brito-Neves, B.B., 2004: Geologia do Continente Sul-Americano: Evolução da obra de Fernando Flávio Marques de Almeida: Beca: São Paulo, p. 595-612.

AUTHORSHIP CONTRIBUTION STATEMENT

Felipe Mature Ribeiro da Silva and Carla Joana Santos Barreto: conceptualization, methodology, validation, and investigation; Sara Gomes da Costa, Jully Vivianne de Albuquerque Alves, Aline Macrina da Silva and Julia Stefane da Silva Vieira: formal analysis and software.

FUNDING SOURCES

This study was carried out with financial support from the PRH 47.1 program, through the Human Resources Project of the Brazilian National Agency of Petroleum, Natural Gas and Biofuels (ANP).